

Copyright Warning & Restrictions

The copyright law of the United States (Title 17, United States Code) governs the making of photocopies or other reproductions of copyrighted material.

Under certain conditions specified in the law, libraries and archives are authorized to furnish a photocopy or other reproduction. One of these specified conditions is that the photocopy or reproduction is not to be “used for any purpose other than private study, scholarship, or research.” If a user makes a request for, or later uses, a photocopy or reproduction for purposes in excess of “fair use” that user may be liable for copyright infringement,

This institution reserves the right to refuse to accept a copying order if, in its judgment, fulfillment of the order would involve violation of copyright law.

Please Note: The author retains the copyright while the New Jersey Institute of Technology reserves the right to distribute this thesis or dissertation

Printing note: If you do not wish to print this page, then select “Pages from: first page # to: last page #” on the print dialog screen

The Van Houten library has removed some of the personal information and all signatures from the approval page and biographical sketches of theses and dissertations in order to protect the identity of NJIT graduates and faculty.

ABSTRACT

PRINCIPLES AND APPLICATIONS OF MECHANICAL DRY COATING - REVIEW AND STATE-OF-THE-ART

**by
Sayani Bhaumik**

Dry Coating of powders to form composite particulates has been firmly established and has garnered interest both in academia and industry due to its myriad applications. This thesis work is an attempt to map the progress of the dry coating technology from its incipient years in the '80s to the thriving practice in the present day. Dry coating is a relatively simple approach to coat powders with specific guest particles via mechanical means to produce composites with desired tailor-made properties, without the constraints of harmful emissions or huge capital investment. Composite particulates with enhanced flowability, high-temperature resistant properties, and modified dissolution characteristics have found its applications in pharmaceuticals, food and agriculture, electrical and automobile sector, cosmetics, ceramics and so on. Besides the Japanese researchers who were the pioneers in this field, considerable impact has been made by our own research group at NJIT. This review is an attempt to benchmark our progress and open up newer research fields yet untapped in the practice of this novel dry coating technology.

**PRINCIPLES AND APPLICATIONS OF MECHANICAL DRY COATING -
REVIEW AND STATE-OF-THE-ART**

**by
Sayani Bhaumik**

**A Thesis
Submitted to the Faculty of
New Jersey Institute of Technology
in Partial Fulfillment of the Requirements for the Degree of
Master of Science in Chemical Engineering**

**Otto H. York Department of
Chemical, Biological and Pharmaceutical Engineering**

May 2015

Blank Page

APPROVAL PAGE

**PRINCIPLES AND APPLICATIONS OF MECHANICAL DRY COATING -
REVIEW AND STATE-OF-THE-ART**

Sayani Bhaumik

Dr. Rajesh Davé, Thesis Advisor Date
Distinguished Professor of Chemical, Biological and Pharmaceutical Engineering, NJIT

Dr. Ecevit Bilgili, Committee Member Date
Associate Professor of Chemical, Biological and Pharmaceutical Engineering, NJIT

Dr. Sagnik Basuray, Committee Member Date
Assistant Professor of Chemical, Biological and Pharmaceutical Engineering, NJIT

BIOGRAPHICAL SKETCH

Author: Sayani Bhaumik
Degree: Master of Science
Date: May 2015

Undergraduate and Graduate Education:

- Master of Science in Chemical Engineering,
New Jersey Institute of Technology, Newark, NJ, 2015
- Bachelor of Technology in Chemical Engineering,
Science College, Calcutta University, Calcutta, West Bengal, India, 2009
- Bachelor of Science in Chemistry,
St. Paul's CM College, Calcutta University, Calcutta, West Bengal, India, 2006

Major: Chemical Engineering

Publications

Z. Huang, W. Xiong, X. Deng, S. Bhaumik, R. Davé, Improved content uniformity of a low dose blend containing a micronized drug after cohesion reduction via dry particle coating, *European Journal of Pharmaceutical Sciences*, Submitted (2015).

J. Scicolone, S. Bhaumik, Z. Huang, L. Gurumuthy, R. Davé, Application of Resodyn Acoustic Mixer in Effective Dry Coating and Consequent Flow Improvement of Pharmaceutical Powders, *International Journal of Pharmaceutics*, Submitted (2015).

To Almighty God for his countless blessings, to my parents Nandita Bhaumik and Asit Kumar Bhaumik to whom I owe my very existence, whose love, affection and guidance has been a beacon in my life, to my little sister Lopamudra Bhaumik for acting like a big sister with her advice and moral support, to my husband Santu Pal for standing by me through thick and thin of life and to all the well-wishers in my family.

ACKNOWLEDGMENT

I would like to express my sincere gratitude to my thesis advisor Dr. Rajesh N Davé for giving me this opportunity to work as part of his research group especially in powder technology. His visionary spirit, guidance and motivation have been an inspiration to me both for this thesis and in life.

I would like to thank Dr. Ecevit Bilgili and Dr. Sagnik Basuray for kindly consenting to be part of my thesis committee.

In addition, I thank Zhonghui Huang whose constant guidance, inspiration and help made this thesis possible. Throughout the year, I have constantly asked her questions and she has helped me patiently all the time.

Thanks to all the members of the research team Dr. Mohammed Azad, Dr. Bhavesh Patel, Dr. Maxx Capece, Lu Zhang, Scott Krull, Meng Li, and Liang Chen and to my friends Kai and Yidong for making my research experience a wonderful and memorable one.

TABLE OF CONTENTS

Chapter	Page
1 INTRODUCTION.....	1
1.1 Background.....	1
1.2 Thesis Outline.....	4
2 THEORY OF DRY-PARTICLE COATING TECHNOLOGY.....	6
2.1 Introduction.....	6
2.2 Modelling of Inter-Particle Adhesive Forces.....	7
2.2.1 Particle Size.....	7
2.2.2 Surface Asperity.....	8
2.2.3 Surface Energy.....	9
2.2.4 Contact Deformation.....	10
2.2.5 Surface Area Coverage.....	11
3 DEVICES USED FOR DRY POWDER COATING.....	13
3.1 Introduction.....	13
3.2 Modern Day Dry Coating Equipment.....	14
3.2.1 Mechanofusion.....	15
3.2.2 Hybridizer.....	16

TABLE OF CONTENTS
(Continued)

Chapter	Page
3.2.3 Magnetically Assisted Impaction Coater (MAIC).....	18
3.2.4 Cyclomix.....	21
3.2.5 Rotating Fluidized Bed Coater (RFBC).....	22
3.2.6 Theta Composer.....	23
3.2.7 Fluid Energy Mill (FEM).....	25
3.2.8 Comil.....	27
3.2.9 Resodyn Acoustic Mixer (LabRAM).....	29
4 CHARACTERIZATION TECHNIQUES.....	31
4.1 Introduction.....	31
4.2 Surface Morphology.....	31
4.2.1 Scanning Electron Microscope.....	31
4.2.2 Transmission Electron Microscope.....	33
4.2.3 Atomic Force Microscopy.....	34
4.2.4 Energy Dispersive X- Ray Spectroscopy.....	34
4.3 Particle Size.....	35
4.3.1 Particle Size Analyzer.....	35

TABLE OF CONTENTS
(Continued)

Chapter	Page
4.4 Flowability Parameters of Powders.....	37
4.4.1 Angle of Repose using Hosokawa Powder Tester.....	37
4.4.2 Hausner Ratio and Carr Index.....	38
4.4.3 FT4 Powder Rheometer.....	40
4.4.4 Flodex.....	51
5 APPLICATION IN PHARMACEUTICAL INDUSTRY.....	53
5.1 Improvement in Flowability of Cohesive Powders.....	53
5.2 Application in Dry Powder Inhaler Technology.....	57
5.3 Modification of Dissolution Profiles.....	59
5.3.1 Enhanced Dissolution.....	59
5.3.2 Controlled Release.....	60
6 APPLICATION OF DRY COATING IN OTHER INDUSTRIES.....	61
6.1 Metal Composites.....	61
6.2 Chromatographic Applications.....	61
6.3 Refractory Materials – Sintering Applications.....	62

TABLE OF CONTENTS
(Continued)

Chapter	Page
6.4 Food and Agriculture.....	63
6.5 Automobile Industry – Automotive catalysts.....	65
6.6 Thermal Insulation.....	66
6.7 Cosmetic Industry.....	67
6.8 Lithium Ion Batteries.....	70
6.9 Paints and Paper.....	70
6.10 Miscellaneous Applications.....	72
7 CONCLUSION.....	78
REFERENCES.....	79

LIST OF TABLES

Table	Page
1.1 Application of Composite Materials	2
3.1 Comminution Devices used in Dry Coating	13
3.2 Powder Mixing Equipment	14
3.3 Some Patented Dry Coating Devices.....	14
4.1 Variation of Flowability with AOR.....	38
4.2 Correlation of CI/HR with Flowability	40
4.3 Correlation of Flowability Index with Flow Behavior	48

LIST OF FIGURES

Figure	Page
1.1 Ordered vs random mixtures	3
1.2 Schematic of dry coating process	4
2.1 Schematic of Rumpf's model.....	8
2.2 Schematic of Xie's model	9
2.3 Different contact scenarios (a) Host-Host (b) Host-Guest (c) Guest-Guest	11
2.4 Adhesion force vs. surface area coverage.....	12
3.1 Schematic of the mechanofusion system.....	15
3.2 Schematic of the hybridizer.....	17
3.3 Schematic of the MAIC.....	19
3.4 Schematic of modelling of dry coating in MAIC.....	20
3.5 Schematic of cyclomix.....	21
3.6 Schematic of rotating fluidized bed coater.....	22
3.7 Schematic of the theta composer (a), (b) and (c) represent different orientations..	24
3.8 Cross-section of the FEM (a), and the milling chamber (b).....	26
3.9 Schematic of the comil.....	27
3.10 Schematic of resonant acoustic mixer.....	29

LIST OF FIGURES
(Continued)

Figure	Page
4.1 SEM micrograph images of cornstarch and alumina.....	32
4.2 TEM micrographs.....	33
4.3 AFM images of selected aluminium particles.....	34
4.4 EDX images of leucine coated with KCl.....	35
4.5 PSD of AlN particles before and after processing with nano-silica in MAIC...	36
4.6 Schematic of aeration test in FT4.	41
4.7 Difference between cohesive and non-cohesive powder (aeration).....	42
4.8 Tapped density in FT4 Powder Rheometer.....	44
4.9 Classification of powders according to flow rates and flow energy.....	45
4.10 Schematic of shear test.....	46
4.11 Relation between shear stress and normal stress.....	47
4.12 Schematic of conditioned bulk density measurement.....	49
4.13 Schematic of compressibility test.....	50
4.14 Schematic of permeability test.....	51
4.15 Flodex.....	52
5.1 Geldart classification of powders.....	54
5.2 Graphic illustration of polymer coating process.....	60
6.1 Schematic of double layer composite particles.....	62

LIST OF FIGURES
(Continued)

Figure	Page
6.2 Schematic illustration of dehydration of food fibre mechano-chemically.....	64
6.3 Application of nano-technology in food sector.....	64
6.4 SEM Images of alumina nano-particles coated on alumina fibre.....	66
6.5 Schematic diagram of glass fibre reinforced fumed silica.	67
6.6 (a) Talc particles (×3200) and (b) Aerosil R972® particles (×12,600).....	69
6.7 Schematic of lithium ion battery.....	70
6.8 SEM of GCC pigment (a), GCC pigment modified with titanium oxide (b).....	71
6.9 Zeta potential (a) non-modified pigments (b) clay modified pigments.....	72
6.10 SEM images of AlN as received.....	73
6.11 AlN coated with 2.0% R972 by MAIC (10 minutes).....	73
6.12 Carbon black XE2 (As received).....	74
6.13 UCF5 CBXE2 1% MAIC coating.....	74
6.14 Copper (As received).....	74
6.15 30 nm Ag (As received).....	75
6.16 30nm Ag-10 Cu-HB-6000rpm-5 mins-2.8%.....	75
6.17 Nano-sized copper (II) oxide.....	75
6.18 CuO-Silver flakes -MAIC (5%).....	76
6.19 Ancamine 2337 (As Received).....	76
6.20 Ancamine 2337 coated with 5% of R972 by MAIC for 15 mins.....	76
6.21 2014FG coated with 50% of R972 by MAIC for 15 mins.....	77

CHAPTER 1

INTRODUCTION

1.1 Background

Dry coating of particles with micron or nano-sized additives to form engineered particulates with tailor-made properties has long been established. Dry coated particles have improved flowability, dispersibility, solubility, color, flavor, taste and even solid-state reactivity(Pfeffer et al., 2001a). Composite particles find its applications in a variety of industries – pharmaceuticals, food and agriculture, ceramics, electrical, automobile, electronics, cosmetics and so on. Table 1.1 summarizes some of the applications of composite materials in various industries(Naito et al., 1993).

Table 1.1 Application of Composite Materials

Application	Host Particle	Guest Particle	Objective
Medicine	Aspirin	Caranuba Wax	Release control of aspirin
	Starch	Indomethacin	Acceleration of indomethacin solution
Cosmetics	Polyethylene Nylon	Pigment Titanium dioxide	Coloring of polyethylene Foundation & UV ray protection
Toner	Resin	Pigment, charge control agent	Fabricate Toners
Electric Conductible Resins	PMMA	Ag	Forming a network of electrical conductible path in bulk materials.
Metals/Ceramics	Al alloy	Y ₂ O ₃	Fabricating interface layer between metal and thermal spray layer.
Thermal Spray Materials	Titanium Nickel	Amorphous Boron Al	Plasma spraying under reduced pressure or in air.
Filler	MgO	Fatty acid	Surface reforming of MgO from hydrophilic to hydrophobic.
Ceramics Filter	Alumina	Zirconia	Fabricating ceramics filter with alkalinity resistance.
Electric Contact Materials	Ag-Ni alloy	Ni	Fabricating rivets with enhanced mechanical strength.

Source: (Naito et al., 1993)

The conventional methods to form composite materials are adsorption, coacervation, film deposition by interfacial polymerization, polymer physisorption, spray drying, chemical vapor deposition and even etching. The disadvantage of the wet coating methods is that it involves the use of toxic solvents which creates unwanted waste and VOC emissions. Gas-phase methods like chemical vapor deposition, physical vapor deposition and sputtering involves generation of vacuum. These conventional methods typically incur huge capital investments and large overhead costs in process equipment.

Dry coating by mechanical means has been firmly established as a viable method to form composite particles in recent years. The concept of dry coating millimeter sized particles with micron or submicron sized particles to reduce van-der-waals attractive forces and other adhesive forces originated from the theory of ordered powder mixing –

pioneered by Hershey and his co-workers (Hersey, 1975). Hersey has defined “ordered mixture” as having zero standard deviation of all the sample concentration at all sample sizes provided the sample size is larger than a single ordered unit as opposed to random mixture where standard deviation decreases with increasing sample size. The term “interactive mixture” has been coined by Sallam et al(Sallam et al., 1986) and is more prevalent in practice. This concept has particularly been useful to the pharmaceutical industry since it reduces segregation and increases homogeneity. One of the methods to mix powders is by shearing forces and this concept has been utilized in mechanical dry coating. In a dry coated composite particle, the guest particle forms a continuous or a discrete layer on the host particle as depicted in Figure 1.2.

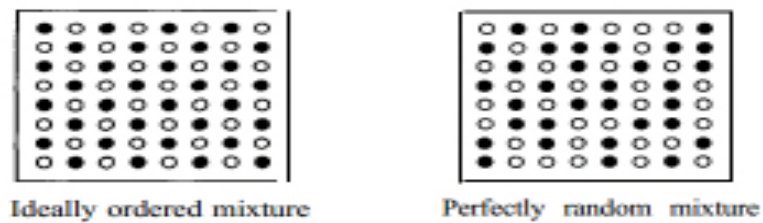


Figure 1.1 Ordered vs random mixture.

Source: (Poux et al., 1991)

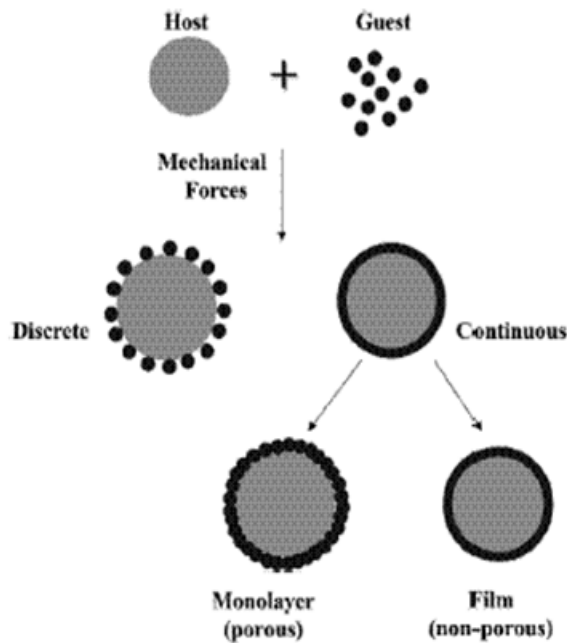


Figure 1.2 Schematic of the dry coating process.

Source: (Pfeffer et al., 2001b)

Japanese researchers have been the front-runners in mechanical dry coating equipment and applications where the comminution techniques and devices like the Angmill and mechanofusion were invented in 1980s. However, since then, this technology has gained ground in the US, spear-headed by our group headed by Prof. Dave at NJIT working in communion with Rutgers and Purdue universities.

1.2 Thesis Outline

This thesis is a review of the applications of dry coating technology in various fields, with a historical perspective and including the latest state-of-the-art trends pioneered by our research group at NJIT.

In chapter 2, all the theoretical models pertaining to dry particle coating technology will be discussed. In chapter 3, the various equipment used in dry particle coating will be discussed. In chapter 4, the various characterization techniques used after dry coating a powder to evaluate the coating effectiveness will be discussed. In chapter 5, the applications of composite materials in pharmaceutical industry will be discussed. In chapter 6, the applications of composite materials in various other industries will be discussed. In chapter 7, the dissertation is concluded with a view to future development.

CHAPTER 2

THEORY OF DRY-PARTICLE COATING TECHNOLOGY

2.1 Introduction

Fine particles are of interest to both academia and industry due to their high surface area. However, these particles often tend to agglomerate and are very cohesive in bulk flow, since their inter-particle van-der-waals forces exceed the gravitational forces. In dry coating, nano-sized guest particles are adhered to the surface of the host particles, as a result they alter the surface morphology of the host particle and in the process the adhesive forces are reduced. The exact mechanism as to why the inter-particle forces are reduced is not yet confirmed and different groups have different viewpoints on the same. Most researchers believe that the guest particles act as spacer particles and increase the intermolecular distance between the host particles(Rumpf and Bull, 1990; Xie, 1997), some of them believe they have a “ball-bearing” or “lubricating effect”(Hollenbach et al., 1983) , some others are of the opinion that they neutralize the electro-static charges of the host particles(Dutta and Dullea, 1990). The reason for this difference is due to the fact that interparticle adhesion force depends on number of factors- particle shape, size, asperity, surface free energy, hardness and elasticity.

2.2 Modelling of Inter-Particle Adhesive Forces

2.2.1 Particle Size

Van der waals forces exist between two constituent particles due to their molecular properties, even if they are electrically neutral. These forces can be attributed to the molecular scale dipole-dipole interactions, dipole-non polar interactions and interactions between non-polar bodies. These forces are quantum mechanical in nature and for an exact expression, rigorous quantum-mechanical electrodynamics is needed. However, a simplified approach is possible, where the interaction force between two molecules a, b, separated by a distance r_{ab} is given by the Lennard-Jones potential.

$$V = -\frac{C_{ab}}{r_{ab}^6} + \frac{D_{ab}}{r_{ab}^{12}} \quad (2.1)$$

The first term in Equation 2.1 is the interaction term, where C_{ab} the London constant and the second term is the Born Repulsion term.

Interparticle adhesion arises as a consequence of attractive forces, which for dry and electro-neutral powders are mainly attributed to van der Waals interaction(Rietema, 1991).

$$F_{ad} \cong \frac{Ad_a}{24z_0^2} \quad (2.2)$$

Here, A is the Hamaker constant, $z_0 \approx 4 \text{ \AA}$ is the intermolecular separation distance, $d_a \approx 0.2 \mu\text{m}$ is the typical surface asperity size. It is to be mentioned here, that the adhesion force can be approximated to the van der waals force, only if deformation at the surfaces can be neglected.

In terms of radius R of the particle, the adhesion force can be expressed as (Bowling and Mittal, 1988),

$$F_{ad} = \frac{AR}{6z_0^2} \quad (2.3)$$

When the deformation is taken into consideration, it becomes more complex, and in a fully plastic regime, the Mauguis-Pollock equation gives an estimate of the inter-particle adhesion force.

2.2.2 Surface Asperity

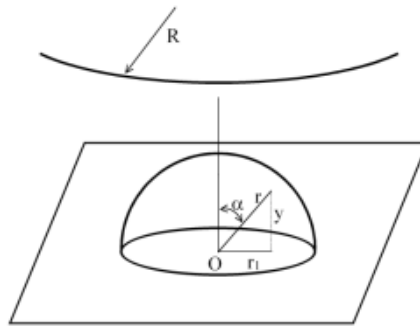


Figure 2.1 Schematic of Rumpf Model.
Source: (Rabinovich et al., 2000)

The Rumpf model is the most widely accepted one to predict the adhesion force considering the effect of nano-scale surface asperity. It is based on the contact between a hemispherical asperities on the centre interacting with a much larger spherical particle along the normal as depicted in Fig. 2.1. Equation 2.4 is the mathematical form.

$$F_{ad} = \frac{A}{12z_0^2} \left[\frac{rR}{r+R} + \frac{R}{(1+r/z_0^2)} \right] \quad (2.4)$$

In this equation A is the Hamaker constant, r is the radius of the asperity and R is the radius of the spherical particle and z_0 is the minimum distance between the particles.

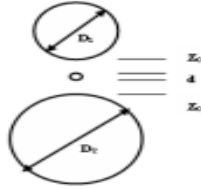


Figure 2.2 Schematic of Xie's model.

Source: (Xie, 1997)

Xie developed a similar approach considering asperity as a small particle in between two large particles. This model given by Equation 2.5 represents the force between two large particles and the force between the smaller particles and two spheres.

$$F_{ad} = \frac{AD'}{12(2z_0 + d)^2} + \frac{A(D'_1 + D'_2)}{12z_0^2} \quad (2.5)$$

Here, $D' = \frac{D_1 D_2}{D_1 + D_2}$, $D'_1 = \frac{D_1 d}{D_1 + d}$ and $D'_2 = \frac{D_2 d}{D_2 + d}$ are the characteristic diameters.

2.2.3 Surface Energy

The inter-particle adhesion force is a short range force, and based on Lennard Jones potential it can be expressed as

$$F(z) = -\frac{8w_{ab}}{3z_0} \left[\left(\frac{z_0}{z} \right)^3 - \left(\frac{z_0}{z} \right)^9 \right] \quad (2.6)$$

Here, w_{ab} is the work of adhesion, z_0 is the equilibrium separation distance z is the equilibrium interatomic distance. The work of adhesion w_{ab} can be expressed as

$$w_{ab} = \gamma_a + \gamma_b - \gamma_{ab} \quad (2.7)$$

Where γ_a and γ_b are the surface free energies of the two interacting solid surfaces, and γ_{ab} is the interfacial energy at the solid-solid interface.

2.2.4 Contact Deformation

The area of contact is important in the calculation of the adhesion force because with larger contact area, more energy is required to create new surfaces. Deformation of contact surface can enlarge the contact area and increase the interparticle pull-off force, defined as the maximum interparticle adhesion force during the separation of two surfaces in contact or the force required to separate two contacted surfaces. Inter-particle pull-off force is a function of the consolidation force and the nature of contact deformation. There may be three types of contact deformation (i) elastic contact (ii) elastic-plastic contact (iii) fully plastic contact.

For elastic contact, Johnson (1971), derived the following expression for adhesion force based on the JKR theory(Johnson et al., 1971).

$$F_{ad} = \frac{3}{2} \pi \Delta \gamma R^* \quad (2.8)$$

Here, $R^* = R_1 R_2 / (R_1 + R_2)$ is the characteristic radius and R_1, R_2 are the radii of individual spheres, and $\Delta \gamma = \gamma_1 + \gamma_2 - \gamma_{12}$ is the work of adhesion between the two surfaces.

Derjaguin et al. (1975) suggested a slightly different expression for the adhesion force based on the DMT model (Derjaguin et al., 1975).

$$F_{ad} = 2\pi\Delta\gamma R^* \quad (2.9)$$

The JKR and DMT models are based on slightly different assumptions and can be correlated by the Tabor parameter. Generally, JKR theory is applicable for soft materials with low surface energy and DMT model for harder materials with higher surface energy.

2.2.5 Surface Area Coverage

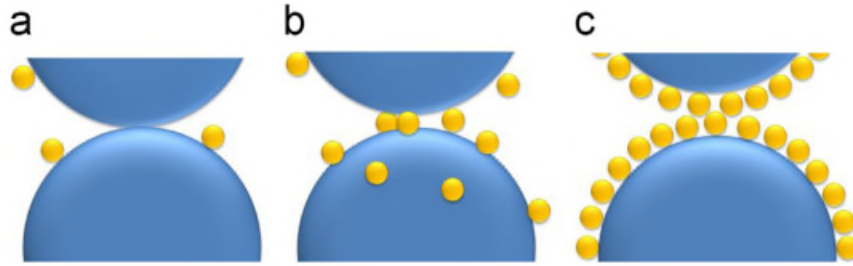


Figure 2.3 Different contact scenarios: a. Host-Host, b. Host-Guest c. Guest-Guest.
Source: (Huang et al., 2015)

Dry coated fine particles can establish a contact between host and host surfaces, guest and host surfaces or guest and guest surfaces depending on the surface area coverage (SAC) of guest particles which is defined as the total projected area of the guest particles on the host particles assuming that the guest particles are distributed evenly on the surface of the host. It is expressed in equation for host- host contact.

$$SAC = \frac{N\pi d^2 / 4}{\pi D^2} * 100\% = \frac{Nd^2}{4D^2} * 100\% = \frac{W_t D^3 \rho_D d^2}{4d^3 \rho_d D^2} * 100\% \quad (2.10)$$

Here, N is the number of guest particles on a single host particle, d is the diameter of the guest particle, D is the diameter of the host particle, ρ_D is the density of the host particle and ρ_d is the density of the guest particle.

Considering a single mono-layer coverage of guest particles on the host particles, and a host-guest contact, SAC can be expressed as,

$$SAC = \frac{N * \frac{\pi d^2}{4}}{4\pi \left(\frac{d+D}{2}\right)^2} * 100\% = \frac{N * d^2}{4(d+D)^2} * 100\% \approx \frac{N * d^2}{4D^2} * 100\% \quad (2.11)$$

The weight percentage of the guest particles for 100% SAC can then be expressed as,

$$Wt\% = \frac{(Nd^3\rho_d)}{(D^3\rho_D) + (Nd^3\rho_d)} * 100\% \quad (2.12)$$

It has been shown by Chen (Chen et al., 2008) that adhesion force decreases with increasing surface area coverage.

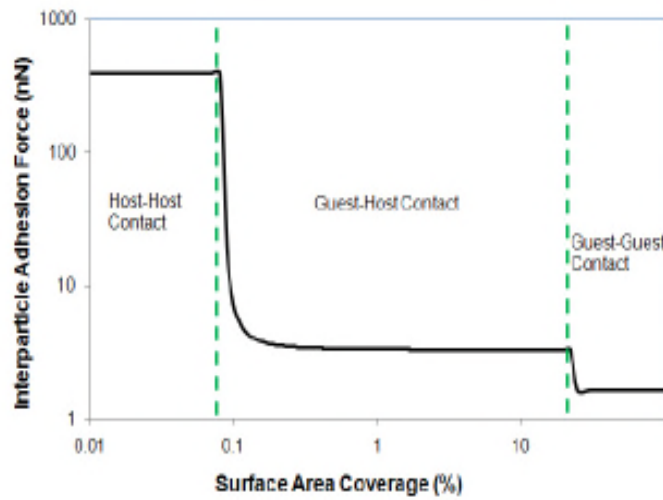


Figure 2.4 Adhesion Force vs. Surface Area Coverage.
Source: (Chen et al., 2008)

CHAPTER 3

Devices used for Dry Powder Coating

3.1 Introduction

Comminution techniques have been applied for dry coating purposes by the Japanese researchers since the 1980s. These machines impart sufficient mechanical forces on the surface of the particles to make composite particles. Some of the important grinding machines that have been used for making composite particles are given in Table 3.1(Naito et al., 1993).

Table 3.1 Comminution Devices used in Dry Coating

Class	Types
Impaction	Pin mill Comminution Devices used in Dry Coating, Disc Mill, and Centrifugal classification type.
Ball Mill	Rotation, Vibration, Planetary, Centrifugal fluidizing type, Jet Mill

Source: (Naito et al., 1993)

Another method which has been used to prepare composite particles is the powder mixing. The powder mixing technology precedes that of dry-coating. Major contributors in powder mixing are Hersey (Hersey, 1975), Egerman and Orr, Moritz, Stainforth, Williams, Cooke, Fan(Fan et al., 1990), Harnby(Harnby, 1967), Oldshue , Alonso (Alonso et al., 1988) to name only a few.

According to Poux (Poux et al., 1991), powder mixing is done by one of the following three processes (i) convection (ii) diffusion and (iii) shear. The shear mixing principle has been used later in dry coating technology. Powder mixing is advantageous in pharmaceuticals since it reduces segregation and increases homogeneity. Powder

mixing equipment some of which has later been used to prepare composite materials are listed in Table 3.2(Poux et al., 1991).

Table 3.2 Powder Mixing Equipment

Mixer	Predominating Mechanism	Applications
Rotating drum	Shear Diffusion	Blending of free flowing granular materials with similar properties.
Double Cone	Shear Diffusion	Blending of dry materials.
Twin Shell Mixture	Shear Diffusion	Blending of dry and free flowing materials.
Ribbon Mixture	Convection	Mixing of dry powders, free flowing materials or flowing pastes and materials which tend to aerate.
Orbitting Screw	Convection, Diffusion	Blending of dry powders, granular materials, creams or pastes.
High Speed Impeller	Convection	To disperse agglomerated materials.
Pan mixer	Shear	To manufacture concrete products.

Source: (Poux et al., 1991)

3.2 Modern Day Dry Coating Equipment

In recent times, specific devices are designed and invented and for dry coating purposes. Some of them apply intense mechanical forces and are classified as hard coating methods. Other devices apply a relatively lower magnitude of force and are classified as soft coating methods. Table 3.3 enlists some of the patented devices for dry coating in use today(Gera et al., 2010).

Table 3.3 Some Patented Dry Coating Devices

Device	Inventor	Company/Institute	US Patent
Mechanofusion	Hosokawa M et al	Hosokawa Micron Corp.	US4789105
Hybridizer	Nara Y, Koishi M	Nara Machinery Co, Ltd.	US4915987
MAIC	Hendrickson WA, Abbott J	Aveka, Inc	US5962082
RFBC	Watano, Pfeffer, Davé	NJIT	US6197369B1
Theta composer	Miyanami K	Tokuja Corp, Japan	US5373999
LabRAM	H.W.Howe et al	Resodyn Corporation	US7188993B1

3.2.1 Mechanofusion

Japanese researchers specifically Yokoyama et al. while working with ultrafine powders and its applications discovered “angmill” or the fine grinding machine to form composite particles(Yokoyama et al., 1983). Later on, Hosokawa Micron Corporation used their principle of using high shear compressive forces to generate particulates and invented a new device named “Mechanofusion”. A schematic of the Mechanofusion device is shown in Figure 3.1.

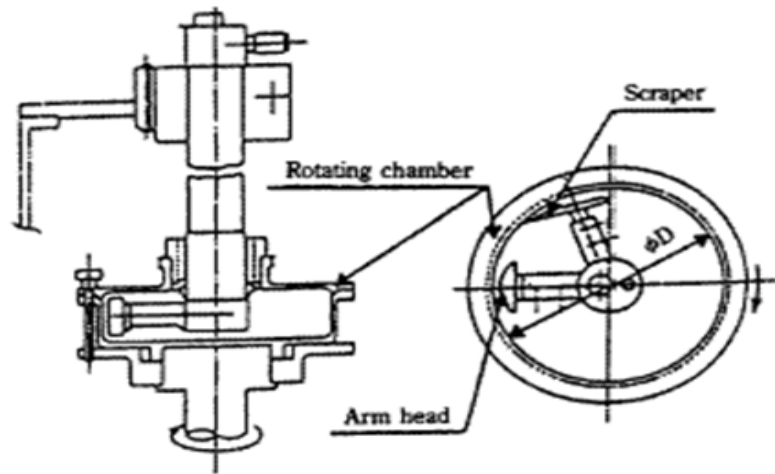


Figure 3.1 A Schematic of the Mechanofusion system.

Source: (Pfeffer et al., 2001b)

The Mechanofusion consists basically of a rotating outer chamber, with a stationary inner piece (press head or arm head), a scraper and a powder inlet and outlet channel. The gap between the inner and outer chamber can be controlled. A measured amount of guest and host particles are fed into the machine, and high shearing and compressive forces fuse the guest onto the host particles. The scraper is used to eliminate any agglomeration and caking. The rotational speed varies between 200 – 10,000 rpm. Strong shearing forces may physically and chemically alter the properties of the materials

associated with some degree of size reduction. This is a batch mode device. The advantages of the device is that it is simple to operate and the high mechanical forces ensures greater degree of coating.

A review on the mechanofusion system and its applications is given by Yokoyama (Yokoyama et al., 1987). In the 1990s leading up to 2001, there has been several research papers on the use of mechanofusion in fuel cells, ceramics, thermal sprays, solid-state alloys, electrodes and so on (Alonso et al., 1989; Farne et al., 1997; Fukui et al., 2001; Herman et al., 1992; Kaga et al., 1990; Nagata et al., 2001; Naito et al., 1990; Tanno et al., 1994; Umakoshi et al., 1993; Wada et al., 1993). In the last decade, leading up to the present days, the application of mechanofusion has been more widespread. Composite particulates prepared by mechanofusion has been used in ceramics(Alvarez et al., 2003; Cooper et al., 2004; Jay et al., 2006; Kato et al., 2002, 2004; Mohan et al., 2003a), preparation of solid oxide fuel cell anode (SOFC) (Fukui et al., 2004; Simner et al., 2006; Simner et al., 2007; Simner et al., 2008), creating humidity resistant magnesium powder(Mujumdar et al., 2004), insulation (Lee et al., 2009; Tay et al., 2012), in improving dry powder inhaler performance by coating the API with lactose and MgSt(Begat et al., 2009; Kumon et al., 2008a; Kumon et al., 2006; Kumon et al., 2008b; Zhou et al., 2013a; Zhou et al., 2010c, 2011) and in delayed release of certain APIs (Hoashi et al., 2013).

3.2.2 Hybridizer

Another group of Japanese scientists led by Honda extended the concept of ordered mixing and designed a high impact dry coating device known as the hybridizer. This

machine was manufactured by Nara Machinery Corp. of Japan. This device is available in various models (NHS-0, NHS-1, NHS-2, NHS-3, NHS-4 and NHS-5) with differing capacities. A schematic of the hybridizer is shown in figure 3.2(Ramlakhan et al., 2000).

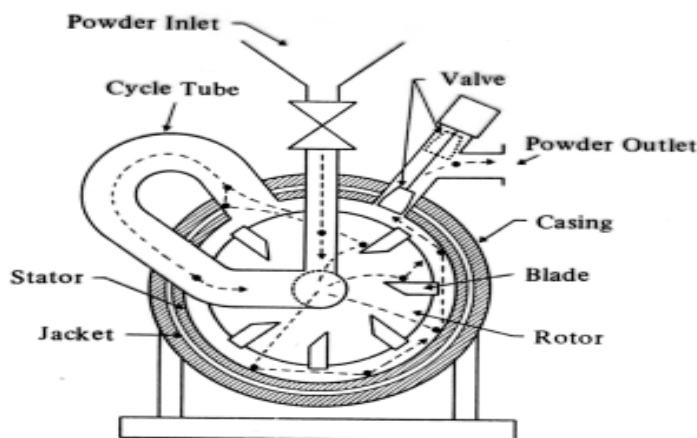


Figure 3.2 Schematic of the Hybridizer.

Source: (Ramlakhan et al., 2000)

This device consists of a very high speed rotor with six blades, a stator, a powder re-circulation tube, and a powder inlet and outlet unit. A heating/cooling jacket is provided for control of local temperature. The guest and host particles are feed into the O.M.dizer (Ordered Mixture dizer; high shear mixer pre-mix system), where the two powders are mixed and dispersed to form an ordered mixture. This mixture is then feed into the hybridizer, where it is subjected to high shear impact and dispersion. The hybridizer disperses the powders and gives them mechanical/thermal energy to embed or coat the guest particles onto the host particles within a very short time (1-5 minutes). This is a batch operated device.

Among the very first research papers on the application of hybridizer is the dissolution of aspirin with potato starch (Ishizaka et al., 1988a), dry coating of sunset yellow with PMMA to obtain sustained release powders (Ukita et al., 1989). At present

hybridizer is used in pharmaceuticals, food, toner, cosmetic industries. Recent papers on the use of hybridization technique include coating of a herbal extract with MgSt for treatment of inflammation (Vilela et al., 2006), dry coating of wheat flour with soyabean hull for reduced fat uptake (Kim et al., 2008; Lee et al., 2008), surface modification of silica gel particles by coating with MgSt (Ouabbas et al., 2009a), enhanced flowability of APIs (Beach et al., 2010), in refractory materials – dry coating of graphite flukes with silica (Ning et al., 2013).

3.2.3 Magnetically Assisted Impaction Coater (MAIC)

The magnetically assisted impaction coater (MAIC), a device developed by the US company Aveka (Aveka Inc., Woodbury, MN 55125) uses relatively lower force to dry coat and hence referred to as a soft coating technique. This method uses a magnetic field to accelerate and spin larger magnetic particles mixed in with the core and guest particles promoting collisions between the particles and with the walls of the device. This results in very good mixing and produces mechanical stresses sufficiently large to promote adherent coating of the guest particles onto the surface of the core particles. A schematic of the MAIC is shown in Figure 3.3.

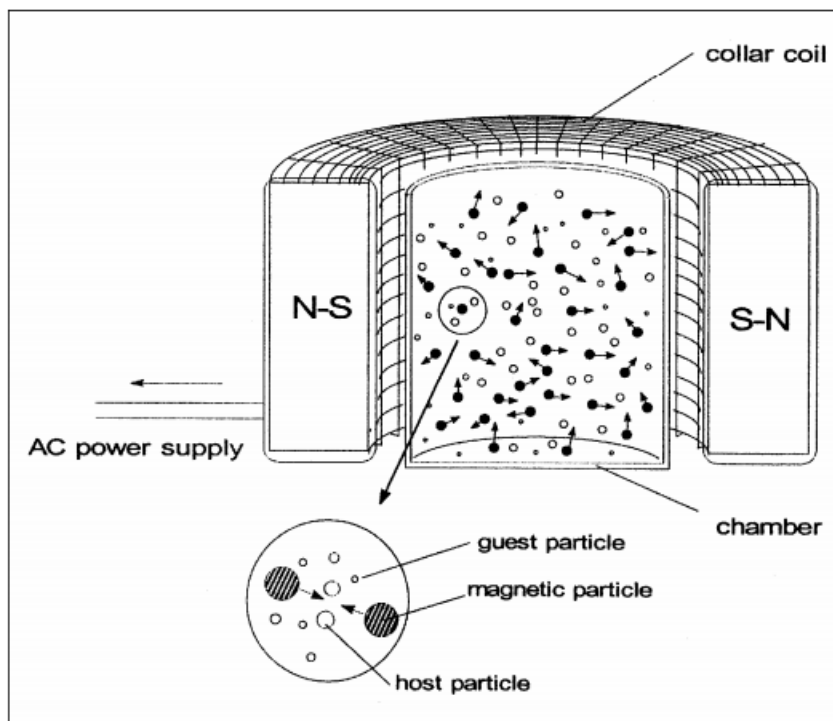


Figure 3.3 Schematic of the MAIC.

Source: (Ramlakhan et al., 2000)

A measured mass of both host and guest particles are placed into a processing vessel 200-ml glass bottle. A measured amount of magnetic particles is also placed in the processing vessel. The magnetic particles are made of barium ferrite and coated with polyurethane to help prevent contamination of the coated particles. An external oscillating magnetic field is created using a series of electromagnets surrounding the processing vessel. When a magnetic field is created, the magnetic particles are excited and move furiously inside the vessel resembling a gas-fluidized bed system, but without the flowing gas. These agitated magnetic particles then impart energy to the host and guest particles, causing collisions and allowing coating to be achieved by means of impaction or peening of the guest particles onto the host particles. The MAIC can be operated in both continuous mode and batch mode which makes it a versatile machine.

The soft coating method is advantageous in the sense that heat sensitive materials can be easily treated.

The earliest known literature on MAIC dates back to 1997 where Prof. R.K Singh showed the use of the device to form composite particulates, $\text{SiO}_2 - \text{SiC}$, $\text{CoO} - \text{Ni}(\text{OH})_2$, $\text{Al}_2\text{O}_3\text{-PMMA}$, $\text{TiO}_2\text{-Al}_2\text{O}_3$ (Singh et al., 1997).Hendrickson showed the use of the device in continuous mode in various applications(Hendrickson and Abbott, 1999). Our own group of researchers at NJIT performed an optimization study on MAIC(Ramlakhan et al., 2000) and later used the device in various dry coating applications like deactivated sintering(Mohan et al., 2003b),improved dispersion of carbon nanotubes by coating with polyethylene oxide(Narh et al., 2008), improvement in flowability of APIs (Ghoroi et al., 2013a; Jallo et al., 2012). Based on the optimization study, a schematic of the proposed mechanism of dry coating is shown in Figure 3.4.

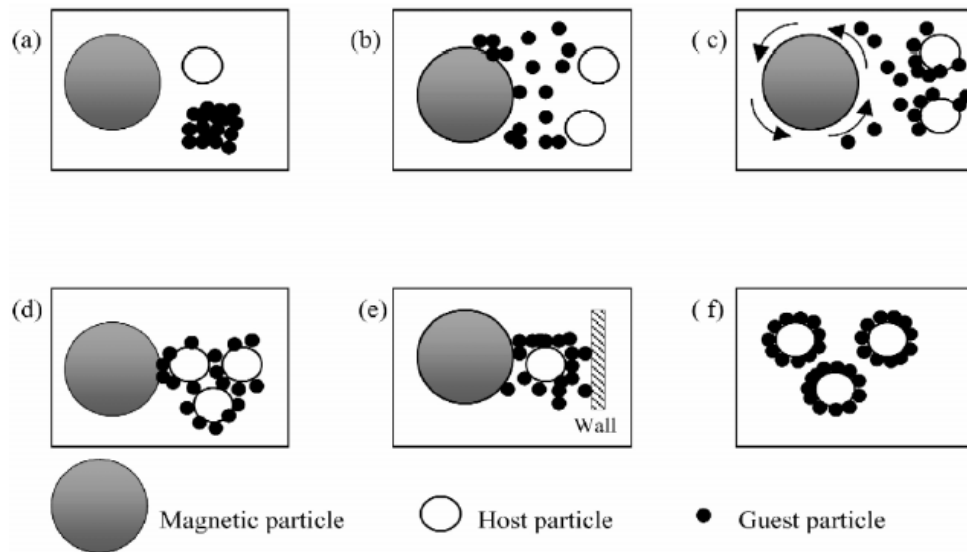


Figure 3.4 Schematic of modelling of dry coating in MAIC.
Source: (Ramlakhan et al., 2000)

3.2.4 Cyclomix

The cyclomix high shear granulator manufactured by the Hosokawa Micron Group is a high speed intensive paddle mixer and agglomerator used for mixing cohesive powders and pastes. A schematic of the cyclomix is shown in Figure 3.5.

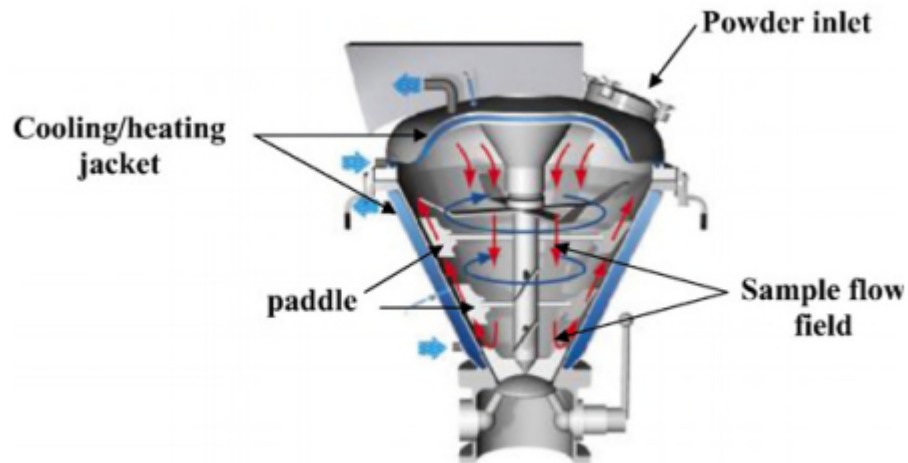


Figure 3.5 Schematic of Cyclomix.

Source: (Ouabbas et al., 2009b).

It consists of a stationary conical mixing vessel having central rotor (speed up to 30 m/s) with mixing paddles, powder inlet/outlet units. A heating/cooling jacket is provided on the casing to control local temperature. The high speed of the rotor creates centrifugal forces and pushes the product to the vessel wall and mixture experiences high shear forces and compressive stresses between wall and paddle. It has good temperature control and the agglomerate size can be effectively controlled. It is available in a variety of sizes from 100 ml to 2000 L of product volume.

The cyclomix high shear mixer was first used for dry coating purposes by Ouabbas et al(Ouabbas et al., 2009b), in dry coating silica gel with varying amounts of

MgSt, and starch with fumed silica. In 2012, Satoh et.al studied the effectiveness of dry coating in cyclomix by investigating the effect of different operating conditions on dry coating sugar grains with MgSt.(Sato et al., 2012).

3.2.5 Rotating Fluidized Bed Coater (RFBC)

At NJIT, a new device was invented within our group, based on the principle of centrifugal fluidization. This device is called the rotating fluidized bed coater (RFBC). It produces soft coatings. A schematic of the RFBC is shown in Figure 3.6.

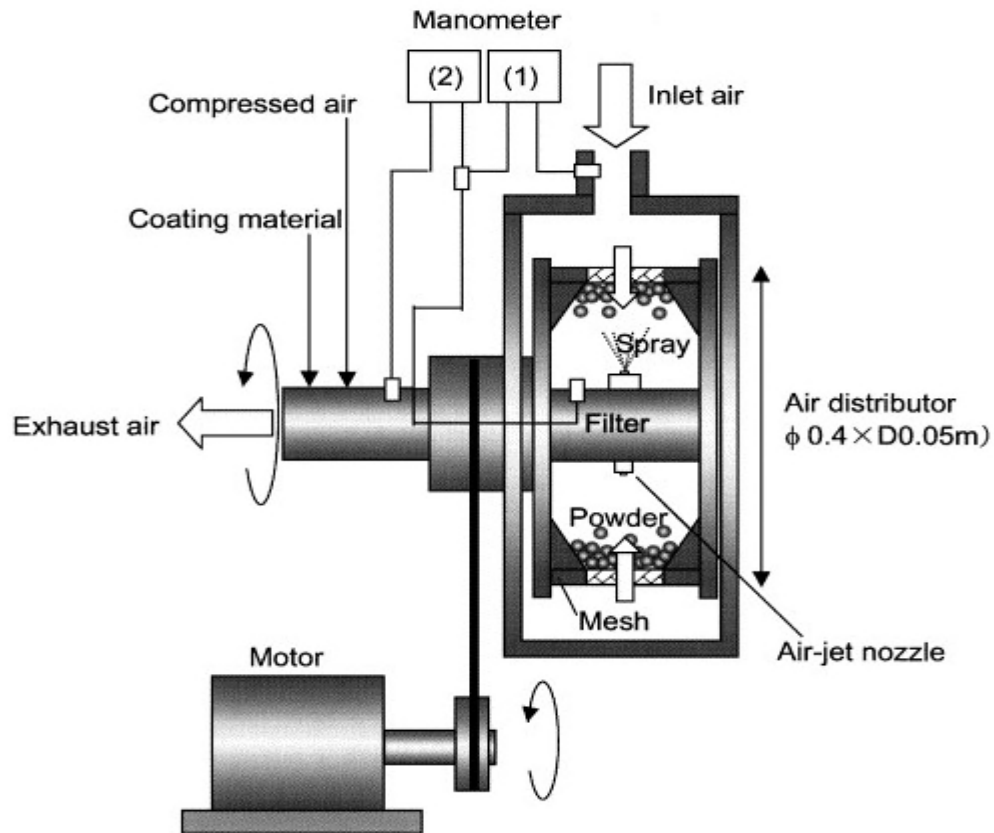


Figure 3.6 Schematic of Rotating Fluidized Bded Coater.

Source: (Watano et al., 2004)

This newly developed coating device operates on the principle of a rotating fluidized bed. The host and guest powder mixture are placed into the rotating bed and is fluidized by the radial flow of gas through the porous wall of the cylindrical distributor. Due to the high rotating speeds, very high centrifugal and shear forces are developed within the fluidized gas–powder system leading to the break-up of the agglomerates of the guest particles. Moreover, the very large flow of air needed to fluidize the particles at high rotating speeds and the motion of bubbles when operating the bed above minimum fluidization conditions. It creates strong mixing and hence good coating is achieved. For example, at 100 g's, the minimum fluidization velocity can be 2 orders of magnitude greater than in a conventional 1g fluidized bed. The RFBC has another advantage over a conventional fluidized bed in that very small host and guest particles belonging to Geldart group C can be easily fluidized by increasing the rotating speed. The RFBC also has the capability of being operated in a continuous mode.

The application of RFBC in dry coating of cornstarch with HPLC is found in our research paper in 2004. (Watano et al., 2004).

3.2.6 Theta Composer

The theta-composer is manufactured by Tokujo Corporation, Japan. It consists of a slow rotating vessel (about 30 rpm) and a faster elliptical rotor (500 – 3000 rpm). A schematic of the theta-composer is shown in Fig. 3.7.

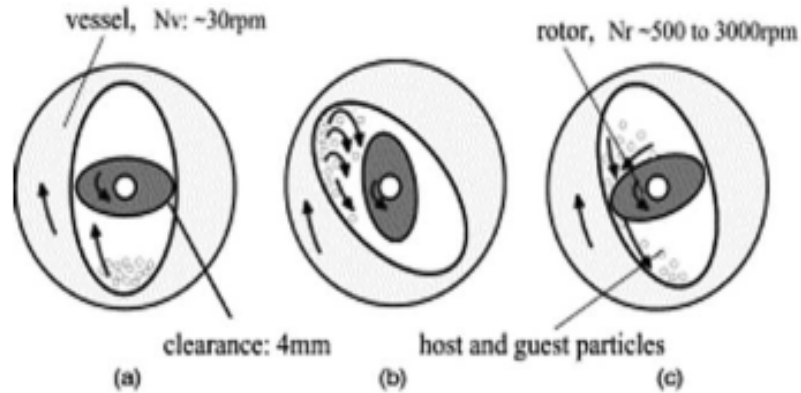


Figure 3.7 Schematic of the theta composer (a), (b) and (c) represent different orientations.

Source: (Pfeffer et al., 2001b)

The outer vessel rotates clockwise and inner rotor rotates anticlockwise in order that the particles are lifted up by the vessel with mixing, and particles receive strong shear stress and compaction forces, when pass through a very narrow clearance between the rotor and the vessel. Due to the strong shear stress and compaction force, a strong coating and composite particles are formed. The critical revolution speed of the particles is given by equation 3.1 (Watano et al., 2000).

$$N_c = \frac{60}{\pi} \sqrt{\frac{g}{2D}} \quad (3.1)$$

The revolution of the outer vessel must be much smaller than the critical speed otherwise the particles will adhere to the walls due to the centrifugal force. Here, D and g represent the inner diameter of the vessel and the acceleration due to gravity respectively.

Japanese literature has the earliest use of theta composer in forming composite fuel cells (Fukui et al., 2003), coating of an inhalation drug with hydrophilic colloidal silica to improve aerosolization (Kawashima et al., 1998b), in dry coating food fibre with

silica (Watano et al., 2000), improving aerosolization of salbutamol sulphate by coating with lactose (Iida et al., 2003a; Iida et al., 2004a; Iida et al., 2004b), in fuel cells (Okawa et al., 2004).

3.2.7 Fluid Energy Mill (FEM)

The fluid energy mill (FEM) manufactured by Sturtevant Inc., Hanover MA 02339 USA, is used in pharmaceutical and food industry primarily for size reduction of micron and sub-micron sized particles. In 1936, the design of the FEM was patented by Norwood H James in the US. A schematic of the FEM is shown in Figure 3.8 (a) and the mill cross-section in Figure 3.8 (b)(Teng et al., 2009). The milling chamber used in our laboratory is 5.08 cm in diameter and 1.27 cm in thickness. The FEM unit includes three air inlets: two grinding air inlets and one feed air inlet. The solid particles are fed into the feed funnel and then sucked into the milling chamber through the Venturi region by the feed air. Sometimes, a volumetric feeder manufactured by Schenck Accurate WI, US, is used to control the solid feed rate. The operating variables that control the operation of the machine are the solid feed rate (SFR), grinding pressure (GP) and feeding pressure. (FP).

The use of the FEM as a simultaneous micronizing and dry coating device was pioneered by Xi Han in our own research group at NJIT. She studied the improvement in flowability by simultaneously micronizing and dry coating ibuprofen with hydrophilic M5P (Han et al., 2011), improved dissolution characteristics and tabletability of blends (Han et al., 2013a) and surface energy studies of milled ibuprofen (Han et al., 2013b).

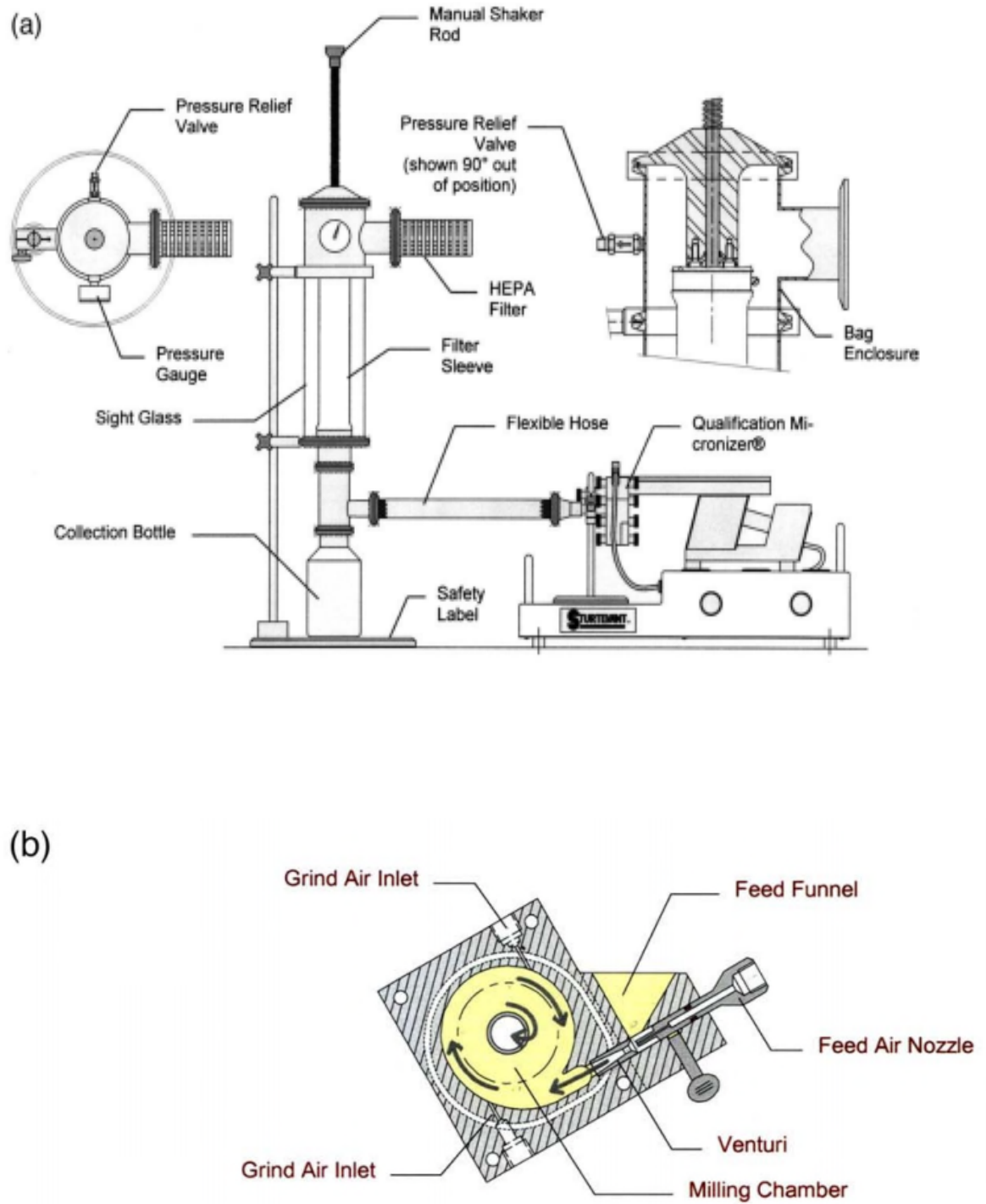


Figure 3.8: Cross-section of the FEM (a), and the milling chamber (b).
 Source: (Teng et al., 2009)

3.2.8 Comil

The conical screen mill or comil as it is commonly called is ubiquitous in pharmaceutical industry. It is manufactured by Quadro Inc., Waterloo, Ontario, Canada. These mills are used for delumping as well as fine control of granule size (Reynolds, 2010). A schematic of the comil is shown in Figure 3.9.

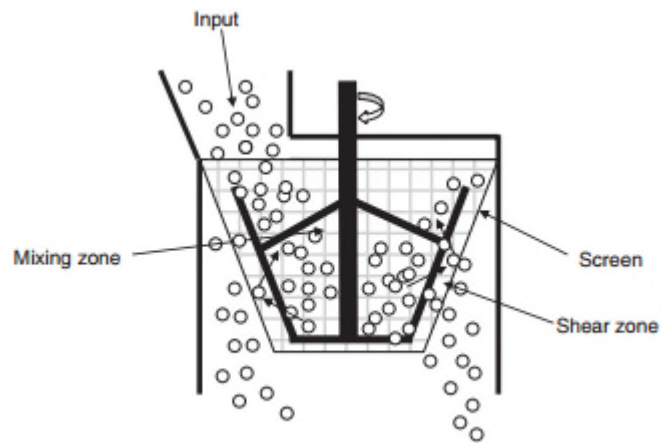


Figure 3.9 Schematic of the Comil.
Source: (Reynolds, 2010)

The key components for a typical conical screening mill are the screen and impeller. They are available with a range of screen sizes, screen types (e.g. round hole vs. rasping) and impeller types (e.g. square edged vs. round edge) and are designed to combine sieving and milling into a single operation. The impeller is typically operated with a variable speed motor, allowing a range of tip speeds to be achieved. A spacer can be used to adjust the distance between the impeller and the screen. Further refinements to this basic configuration can also be adopted. Dry powder coating was achieved using a conventional comil to exploit its capability for deagglomeration with intensified mixing. As powder is charged to the mill, it is retained and mixed in the middle of the conical

vessel. The conical design and centrifugal forces propel the mixed particles outward and up toward the impeller tip and screen. As the particles become trapped between the screen and impeller edge, significant shear stresses are imparted to de-agglomerate the silicon dioxide particles. It is believed that during this time period the larger agglomerates of nano-sized silicon dioxide particles break-down into smaller sub-agglomerates and preferentially attach to the substantially larger host particles through van der Waals attractions. Further residence time is expected to promote repeated collisions between larger host particles having some sub-agglomerates attached and this would lead to transfer/redistribution of nano-particles ultimately resulting in uniform coating of nano-particles. After shearing, some of these coated particles pass through the screen open area and the remaining contained particles are displaced back into the center mixing zone. Eventually all of the particles pass through the screen until the entire charge volume is emptied. This design of the comil enables it to be used as a batch or continuous unit operation. This process requires the selection of comil operating conditions (screens, impeller, operating speed and the powder feeding rate) that are specific to the powder as to maximize dispersion and enable throughput without screen blinding.

The use of comil as a dry coater has been exploited by researchers in our group at NJIT (Huang et al., 2015; Mullarney et al., 2011a) and elsewhere(Chattoraj et al., 2011).

3.2.9 Resodyn Acoustic Mixer (LabRAM)

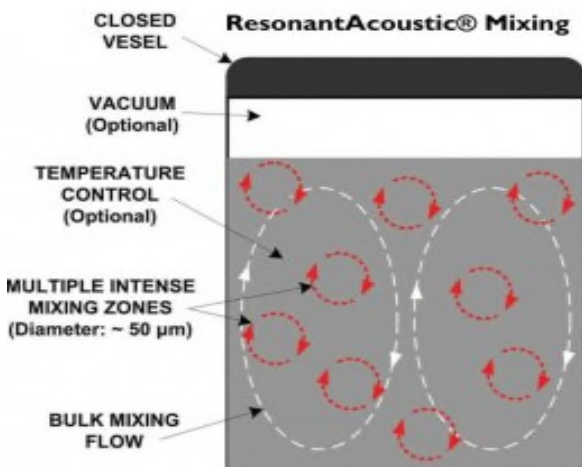


Figure 3.10 Schematic of Resonant Acoustic Mixing.

Source: <http://www.resodynmixers.com>

A schematic of the LabRAM is shown in Figure 3.10. The LabRAM is a sophisticated bench top mixer which uses the resonant acoustic technology which creates a low frequency, high intensity shear field which helps in uniform mixing of the material within relatively short time. Due to the intense vibration of the process, guest particles were able to disperse and adhere to the surface of the host particles creating a uniform layer. The vibration intensity and mixing time can be varied, by external digital controls. The automatic frequency of vibration is normally between 50-65 Hz. The acceleration is the primary parameter that promotes mixing in the LabRAM. This device uses acoustic energy, in the form of intense vibrations, to create high shearing zones within the mixing vessel. This high energy creates an almost fluidized state for the powders and in the process the submicron sized guest particles collide with the host particles, resulting in dry coated host particles.

Research papers on the use of RAM as an effective dry coating device are relatively recent(Capece et al., 2014; Mullarney et al., 2011b), and our group has made valuable contribution to it.

CHAPTER 4

CHARACTERIZATION TECHNIQUES

4.1 Introduction

Particle characterization is extremely important in dry coating technology since it is characterization alone that helps us determine the efficiency of dry coating. Dry coating is done to accomplish a variety of purposes – the most pronounced among them is the improvement in flowability. However, the characterization method will depend on the purpose, for which the coating is done, for flowability improvement, flow properties are studied, for change in dissolution characteristics, dissolution profiles are studied, for improvement in wettability, angle of contact is important. The common factor among them is that the surface is modified in all the cases; hence, study of the morphology is crucial in all instances.

4.2 Surface Morphology

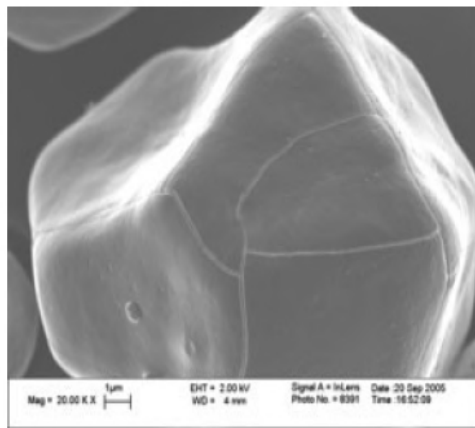
The most common tools to study the surface morphology of dry coated powders are the scanning electron microscope and the transmission electron microscope.

4.2.1 Scanning Electron Microscope

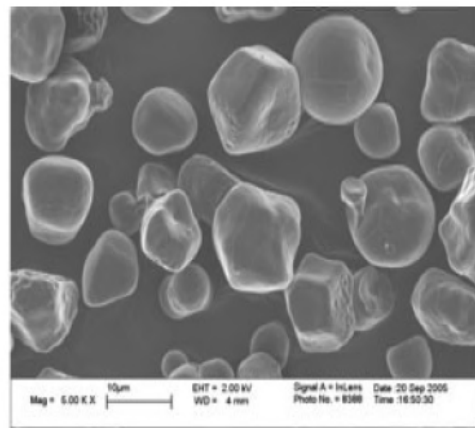
The scanning electron microscope is a common tool used to study the characteristics of the surfaces, under different pressures and different conditions (wet and dry). In our

laboratory, the LEO 1530 VP field emission scanning electron microscope is used. The FESEM was operated at accelerating voltages of 10 – 20 KV either in secondary electron emission (SE) mode or back scattered electron emission (BSE) mode depending on the samples studied.

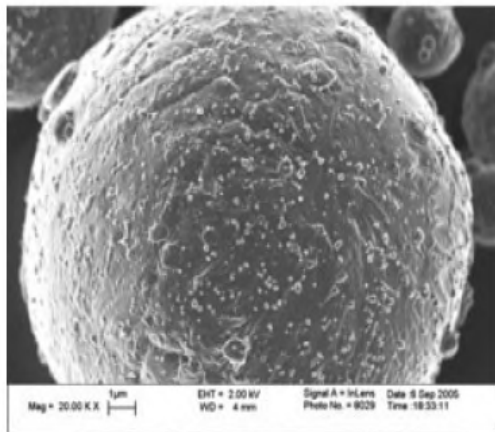
The figures A and B represent cornstarch at magnification of 20,000 and 5000 times and C and D represents 10 -14 μm aluminium at the same magnification.



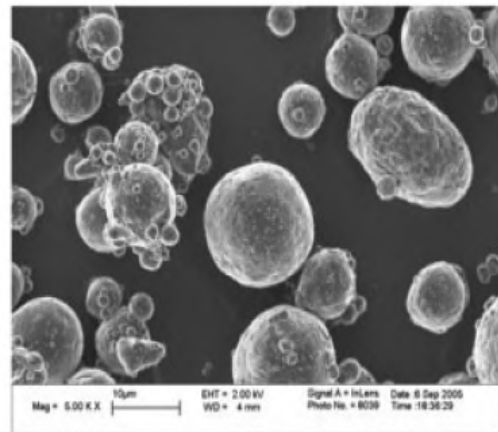
A



B



C



D

Figure 4.1 SEM micrograph images of cornstarch and alumina.
Source: (Chen et al., 2008)

4.2.2 Transmission Electron Microscope

Transmission electron microscopy (TEM) is a microscopy technique in which a beam of electrons is transmitted through an ultra-thin specimen, interacting with the specimen as it passes through. An image is formed from the interaction of the electrons transmitted through the specimen; the image is magnified and focused onto an imaging device, such as a fluorescent screen, on a layer of photographic film.

In our lab, a 200 kV Phillips CM20 Transmission Electron Microscope equipped with a Schottky field-emission source (Wei et al., 2002).

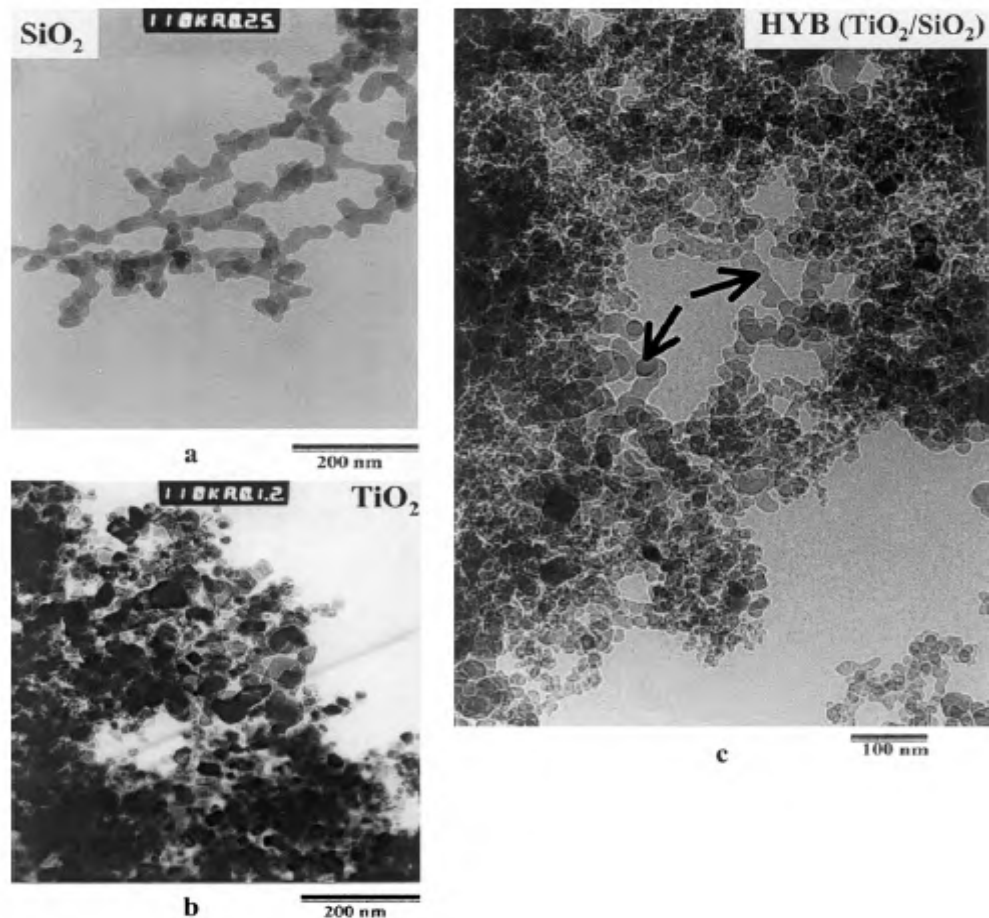


Figure 4.2 TEM micrographs of silica (a) and titania (b) and composite (c).
Source: (Wei et al., 2002)

4.2.1 Atomic Force Microscopy

Atomic Force Microscopy Nanoscope IIIa (Veeco, USA) is employed to assess the surface roughness in tapping mode. In addition to surface morphology, the phase imaging mode of the AFM can, in principle, be used to detect variations in composition, adhesion, friction, viscoelasticity, and other properties of the mixture. The AFM images of aluminium particles are shown in Figure 4.3(Chen et al., 2010b).

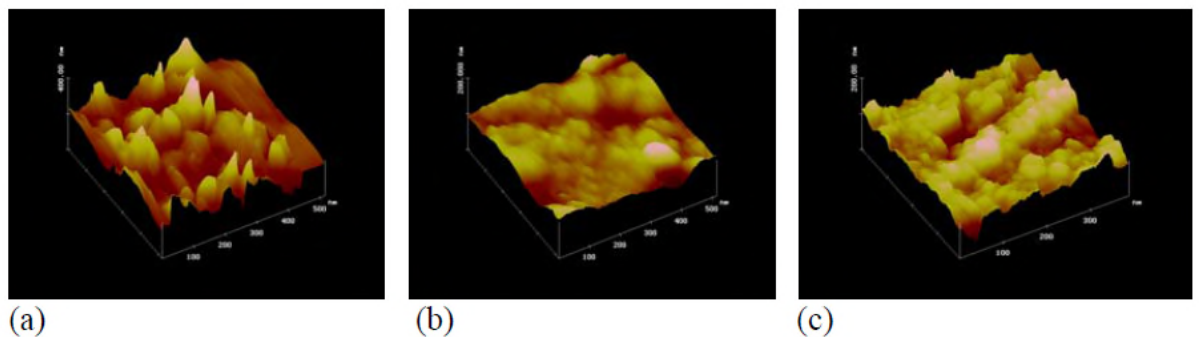


Figure 4.3 AFM images of selected aluminium particles.
Source:(Chen et al., 2010a)

4.2.2 Energy Dispersive X- Ray Spectroscopy

EDS is employed to analyze the chemical composition of the surface of a mixture. The spectra were collected using a LEO Field Emission Scanning Electron Microscope equipped with an Oxford UTW X-ray detector. The following figure depicts the EDX mapping of leucine dry coated with KCl.

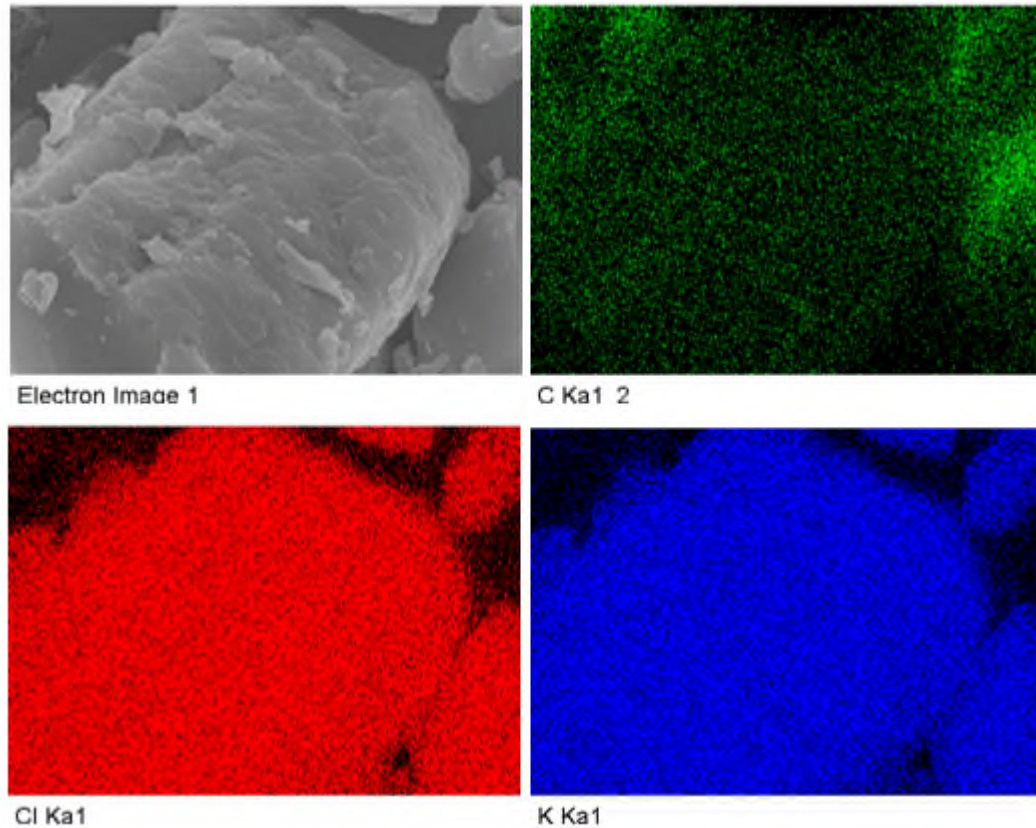


Figure 4.3 EDX images of leucine coated with KCl.

Source: (Ghoroi et al., 2013b)

4.3 Particle Size

In powder technology, one can predict powder behavior if one can measure particle size and shape. Hence, particle size or rather particle size distribution is ubiquitous in all powder technology papers.

4.3.1 Particle Size Analyzer

Particle size and size distribution of the powders were measured in a Rodos/Helos unit (Sympatec, NJ, USA). The instrument has a powder dispersion component which works on the venture principle (RODOS) and a laser diffraction component (HELOS) with a

parallel laser beam of 632.5 nm to measure particle sizes ranging from 0.1 μm to 3500 μm . The HELOS operating principle is based on the Fraunhofer Enhanced Evaluation (FREE) and Mie Extended Evaluation (MIEE) theories of light scattering. When in operation, the RODOS, through the expansion of compressed air accelerates the powder sample and causes dispersion by (1) particle–particle collisions, (2) particle–wall collisions, and (3) centrifugal forces due to strong velocity gradients. The dispersed aerosol is blown through the laser beam, analyzed by the HELOS and collected by suction using a vacuum. In addition, pressure titration tests were performed by a series of repeated measurements at different dispersion pressures from 0.2 bar to 3.0 bar to study the powder dispersion and attrition due to dry coating.

At NJIT, aluminium nitride and boron nitride were coated with nano-silica to (1) to increase the filler loading capability to increase thermal conductivity; (2) to stabilize the fillers surface and (3) to increase the thixo index. Figure 3.4 depicts the particle size distribution of AlN before and after coating in MAIC.

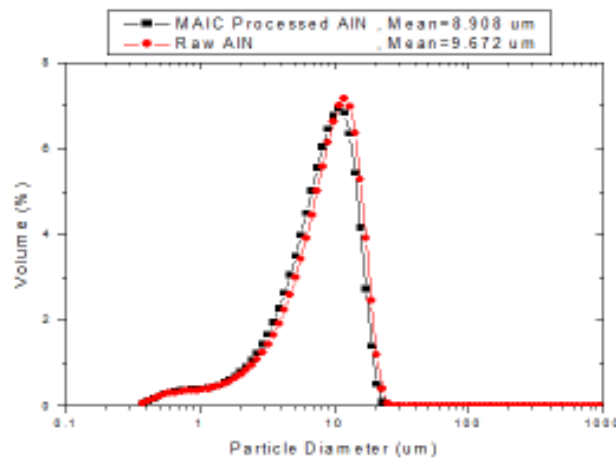


Figure 4.5 Particle Size distribution of AlN particles before and after processing with nano-silica in MAIC.

4.4 Flowability Parameters of Powders

Powder flowability is a complex phenomenon which depends on particle size (Molerus and Nywlt, 1984), shape, moisture content, vessel geometry (Li et al., 2004), and materials characteristics (Vasilenko et al., 2011), such as surface texture, surface energy, chemical composition, and packing and particle–particle interactions (Guerin et al., 1999). Flowability classification of powders is proposed by Heisted (Hiestand, 1991; Hiestand and Smith, 1991) in terms of excellent, good, poor, and very poor based on Carr Index (Carr, 1965) and Hausner ratio (Hausner, 1967). Guerin et al. (Guerin et al., 1999) characterized different pharmaceutical powders using mercury porosimetry, tapped density and shear test. They correlated Carr Index vs. Jenike Indices and compressible volume vs. applied pressure measured by mercury porosimetry. Thus, understanding of powder flow requires number of flow testers. Thalberg and his colleagues (Thalberg et al., 2004) is one of the few researchers who did a comparison of different flow tests.

In this review, some of the commonly used flow tests are summarized below.

4.4.1 Angle of Repose using Hosokawa Powder Tester

The angle of repose of a granular material is the steepest angle of descent or dip relative to the horizontal plane to which a material can be piled without slumping. At this angle, the material on the slope face is on the verge of sliding. The angle of repose can range from 0° to 90°. Lower the angle of repose greater the flowability of the powder. The powder flow properties along with the corresponding angle of repose are given in Table 4.1.

Table 4.1 Variation of Flowability with AOR

Flow Property	Corresponding Angle of Repose (in degrees)
Excellent	25 ⁰ -30 ⁰
Good	31 ⁰ -35 ⁰
Fair- aid not needed	36 ⁰ -40 ⁰
Passable - may hang up	41 ⁰ -45 ⁰
Poor - must agitate, vibrate	46 ⁰ -55 ⁰
Very Poor	56 ⁰ -65 ⁰
Extremely Poor	>66 ⁰

Source: US Pharmacopeia 29.

The powder was loaded into a sieve on a vibration plate. The powder flows through the sieve and down the funnel for 180 seconds. The powder forms a conical pile onto a circular plate. The angle between the surface of the powder heap and the surface of the plate is measured with the measuring pin by aligning it parallel to the surface of the powder. The measurement was performed according to the ASTM standard ASTM D6393-99 “Bulk Solids characterization by Carr Indices,” using the Hosokawa powder tester (PT-N Powder characteristic Tester, Hosokawa Micron Powder System Co., Summit, NJ, USA). For each powder, the procedure was repeated and an average value was reported as the AOR.

4.4.2 Hausner Ratio and Carr Index

The Hausner ratio and the Carr index are widely used parameters to quantify the flow characteristics of the powder. Hausner Ratio given by equation 3 is defined as the ratio of tapped density (ρ_t) to the bulk density (ρ_c). Hausner ratio decreases with the decrease in cohesivity of powder (Dutta and Dullea 1990). According to Geldart et al., the Hausner

Ratio is a good indicator of fluidization behavior of powders. Its range is generally as follows:

- $HR > 1.4$: powder is classified as Group C;
- $HR < 1.25$: powder is classified as Group A;
- $1.25 < HR < 1.4$; powder may show behaviors of both the groups.

Similar to HR, another important index based on freely settled and tapped densities (TD) is Carr index (CI). CI is defined as the coefficient obtained from the difference between TD and freely settled density divided by TD, given by equation 4. It is also known as compressibility index. It was introduced by Carr (1965) to characterize the flowability of bulk solids using a scale of 0-100. A powder that has a CI greater than 25 is considered poor flowing while well flowing powders have a value less than 15. Since the freely settled density can vary greatly due to trapped air within the powder bed, the conditioned bulk density (ρ_c) was used. The generally accepted scale of flowability according Hausner Ratio and Carr Index is given in Table 5 (USP 29).

$$HR = \frac{\rho_t}{\rho_c} \quad (4.1)$$

$$CI = 100 * \left(\frac{\rho_t - \rho_c}{\rho_c} \right) \quad (4.2)$$

The tapped density was measured by tapping a graduated cylinder containing the powder of known volume. The Sotax tapped density tester (Sotax, Switzerland) was used according to the USP II standards to measure the tap density of the powders and the

results reported were the average of three runs. The powders were first placed into a graduated cylinder and mounted on a tapping platform. The cylinders were tapped in increments of 500 taps up to 1500 taps or until no further change in the volume of the powder in the graduated cylinder was observed.

Table 4.2: Correlation of CI/HR with flowability

Compressibility Index (%)	Flow Character	Hausner Ratio
<10	Excellent	1.00-1.11
11-15	Good	1.12-1.18
16-20	Pair	1.19-1.25
21-25	Passable	1.26-1.34
26-31	Poor	1.35-1.45
32-37	Very poor	1.46-1.59
>38	Extremely poor	>1.60

4.4.3 FT4 Powder Rheometer

The FT4 Powder Rheometer manufactured by Freeman Technology Limited, Worcestershire U.K. uses patented technology, a fully automated shear cell and various bulk properties like bulk density, compressibility and permeability to quantify powder flow and processability.

4.4.3.1 Aeration. In order to quantify the influence of air, a controlled air supply can be introduced through a porous mesh at the base of the powder column. This method is not just to simulate processes and applications where air is intentionally introduced into the powder, such as during conveying, drying and in dry powder inhaler applications, but importantly to explore the cohesive forces that exist between particles.



Figure 4.6 Schematic of Aeration Test in FT4.

Source: <http://www.freemantech.co.uk>

Cohesive forces are notoriously difficult to measure, but can now be accurately and directly quantified by assessing how aeration changes the flow properties of the bulk powder. Cohesive forces are a combination of Van der Waal’s and electrostatics, and tend to “bond” particles together. The introduction of air to the powder column attempts to separate adjacent particles and overcome these cohesive forces. If the forces are weak,

each particle will become mechanically separated from its neighbor and the powder will become fluidized. The measured resistance to flow, the *Aerated Energy*, AE quantifies the strength of the cohesive forces.

For powders with weak cohesive forces, the Aerated Energy tends towards zero as the powder becomes fully aerated. Powders with moderate to high cohesion will exhibit a reduction in flow energy when aerated, but to a much lesser extent. In these cohesive powders, the tensile forces are too strong for the air to overcome and the particles do not separate. Instead a channel is established in the powder through which the air passes, and the corresponding Aerated Energy remains relatively high, even at high air velocities.

Contrasting Basic Flowability Energy with Aerated Energy results in the *Aeration Ratio*, AR , where: -

$$\text{Aeration Ratio}_{xx} = \text{Basic Flowability Energy} / \text{Aerated Energy}_{xx} = \text{BFE} / \text{AE}_{xx}$$

where 'xx' defines the air velocity in mm/s at which the Aerated Energy measurement is taken. The Aeration Ratio is a measure of the powder's sensitivity to aeration.

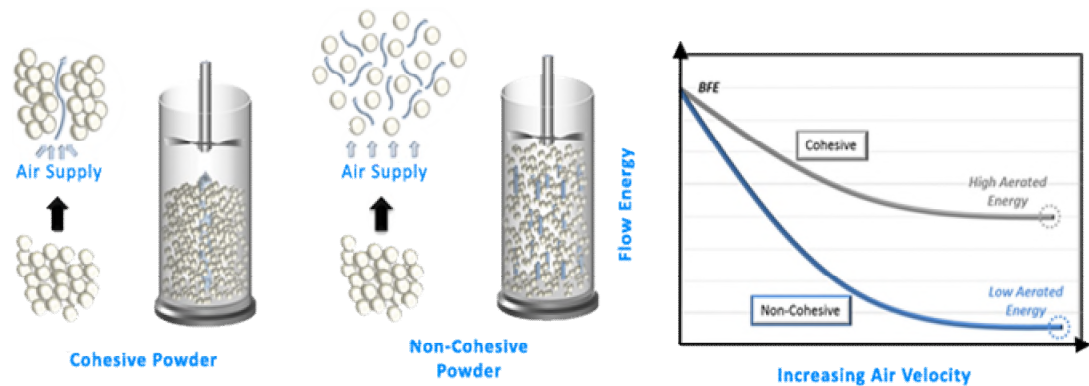


Figure 4.7 Difference between cohesive and non-cohesive powder (aeration)

Source: <http://www.freemantech.co.uk>

4.4.3.2 Consolidation. The effect of consolidation on flow properties can be directly quantified by the *Consolidation Energy, CE*. This is a very similar test to the Basic Flowability Energy, but is completed on a powder sample that has first been subjected to a level of consolidation. Like the BFE method, the flow energy is determined as the blade moves through the powder sample from the top to the bottom. Initially a Conditioning cycle is employed to generate a uniform packing density, before the powder is subjected to a number of taps, in order to induce consolidation in the sample, prior to it being measured. The resulting increase in resistance to flow is quantified by the Consolidation Energy.

It is also possible to consolidate the powder using an applied normal force. This compaction technique more closely simulates how powders would behave during storage, in contrast to behavior during transport or in other environments where they are subjected to vibration. In both methods, the powder is first consolidated before the flow energy is measured.

Contrasting the Consolidated Energy with the Basic Flowability Energy provides a relative change in the powder's flow properties as a function of consolidation. It is a measure of the powder's sensitivity to consolidation and is expressed as the *Consolidation Index, CI*, where: -

Consolidation Index, $CI_{xx} = \text{Consolidation Energy}_{xx} / \text{Basic Flowability Energy} = CE_{xx} / \text{BFE}$

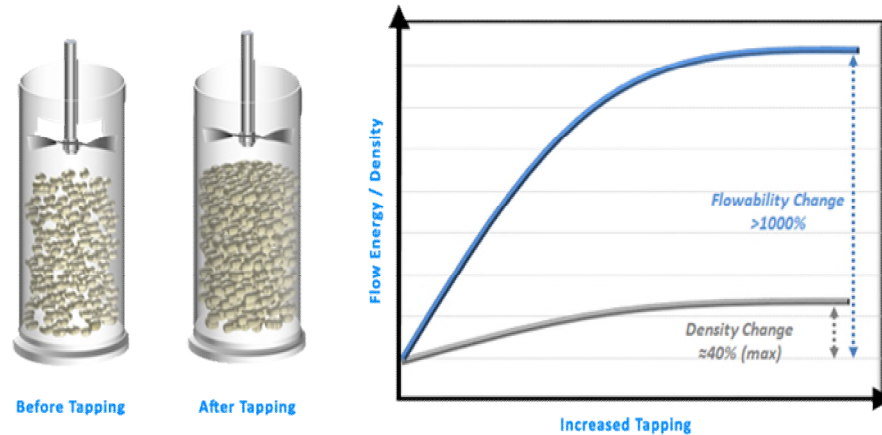


Figure 4.8 Tapped Density in FT4 Powder Rheometer.

Source: <http://www.freemantech.co.uk>

Traditional tapped density based methods, such as Carr's Index and Hausner Ratio, seek to define certain aspects of powder flowability based on a volume change, as a result of tapping the sample. As the graph above illustrates, changes in density may be as high as 40%, however flowability may actually have changed by 1000% as a consequence of tapping. This direct measurement of Consolidated Energy quantifies that the flow properties are in fact 10 times worse after tapping and illustrates why inferring flow characteristics from density measurements is often misleading. After all, from a processing and application perspective, the interest is mostly to determine whether the product will flow, rather than whether its density has changed.

4.4.3.3 Flow (Shear) Rate Sensitivity. Powders typically exhibit different flow behavior when moved at different flow rates. This means that they may flow freely at one speed and badly at another. This sensitivity to changes in flow rate has a number of implications for powder processors and can seriously effect process stability.

Unlike many liquids, powders are rarely Newtonian in nature, exhibiting a complex behavioral relationship with the speed at which they flow. In fact it is common

that powders are more difficult to move at lower speeds than at higher velocities, meaning that if a process is subject to variation in the rate powder moves through it, blockages may occur should flow rates drop below a critical value.

In addition, powders with high flow rate sensitivity will require an optimized and specific mixing configuration if blend uniformity is to be attained. The advantage of powders with low flow rate sensitivity is that low shear mixing operations can be employed, whilst still ensuring homogeneity, minimizing the chances of particle attrition and electrostatic charge evolution which are commonplace in high shear blending. Powders exhibiting high flow rate sensitivity normally require high shear processes in order to blend efficiently.

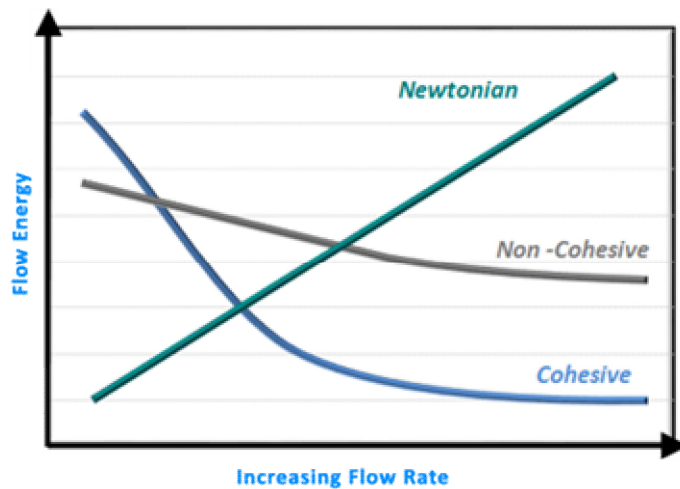


Figure 4.9 Classification of Powders according to flow rates and flow energy.

Source: <http://www.freemantech.co.uk>

4.4.3.4 Shear Cell. The FT4 also includes a Shear Cell accessory which allows the powder's shear properties to be quantified. Shear testing is a very different technique to

that of dynamic testing, and always characterizes the powder in a consolidated state. It is also a fairly static test, measuring the powder's behavior as it transitions from no-flow to flow.

For these reasons, it is clear to see why shear cells are ideally suited to predicting powder behavior in process operations where the powder is consolidated and where flowrates are low and / or sporadic. They have been successfully applied for understanding powder behavior in hoppers, and also provide some of the data needed to carry out a hopper design exercise (based on Jenike stress theory developed during the last century). However, as a consequence of the regime in which they operate, they are less suited to predicting powder behavior in low stress or dynamic applications, such as mixing, filling, feeding and conveying.

Operating Principle

At very low speeds, a shear (or horizontal) force is applied to an upper layer of powder whilst the adjacent lower layer is prevented from moving (or visa-versa). The force continues to increase but no relative movement at the shear plane occurs until the shear force is sufficiently high to overcome the powder's shear strength, at which point the powder bed 'yields' and the upper layer of powder slips against the lower.

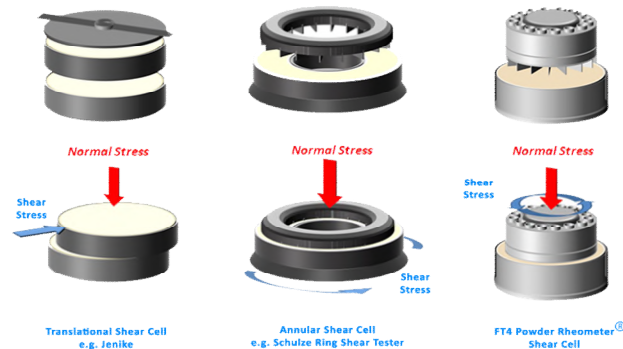


Figure 4.10: Schematic of Shear Test

Source: <http://www.freemantech.co.uk>

Several types to shear cell design have emerged over the last 50 years, however each employs the same concept of shearing one layer of powder against the other. The designs most frequently in use today are rotational in nature, and are preferred as they allow the two layers of powder to be sheared relative to one another over a large distance, in contrast to translational designs that quickly exhaust their range of displacement.

In a typical shear cell test sequence, several shear tests would be carried out at different levels of normal stress. The data produced represents the relationship between shear stress and normal stress, which can be plotted to define the powder's Yield Locus. In simple terms, the higher the shear stress for a given normal stress, the less likely it is that the powder will yield and begin to flow when confined under a similar consolidation stress in a hopper or other vessel.

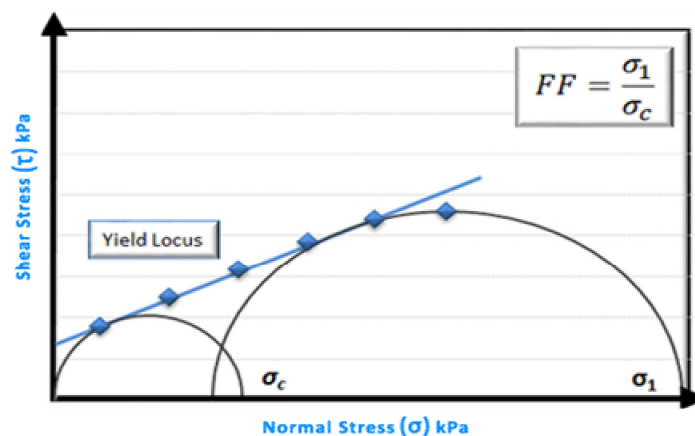


Figure 4.11 Relation between shear stress and normal stress.

Source: <http://www.freemantech.co.uk>

It is possible to apply a number of mathematical models to this data, but it is important to consider that in doing so, trends may be exaggerated or reduced. Fitting

Mohr stress circles to the yield locus identifies the *Major Principle Stress* (σ_1) and *Unconfined Yield Strength* (σ_c), and the ratio of the former to the latter quantifies the *Flow Function, FF*. Flow Function is a parameter commonly used to rank flowability, with values below 4 denoting poor flow and above 10, good flow.

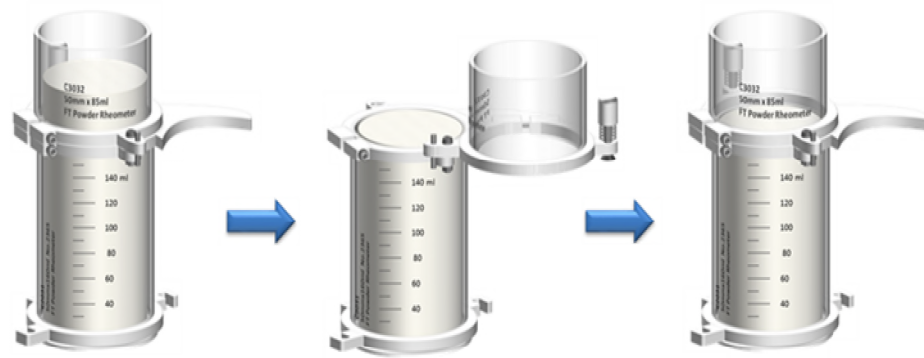
Table 4.3 Correlation of flowability Index with flow behavior

Flowability Index	Flow Behavior
Ffc	
$ffc < 1$	Not Flowing
$1 < ffc < 2$	Very Cohesive
$2 < ffc < 4$	Cohesive
$4 < ffc < 10$	Easy-flowing
$10 < ffc$	Free Flowing

4.4.3.5 Bulk Properties. Bulk properties are not a direct measurement of flowability or shear, but nevertheless influence process performance and product attributes. The FT4 measures typically three types of bulk properties: -

Density

Density defines the relationship between mass and volume. In principle this seems a simple concept, but the nature of powders means that their packing structure can change easily and significantly. Therefore when defining density, it is essential to ensure the packing state is well known and can be reproduced. This is achieved on the FT4 using a conditioning cycle. When combined with other features such as the built in balance and Split Vessels, which allow a precise volume to be attained, the Conditioned Bulk Density can be measured with unprecedented levels of accuracy.



$$\text{Conditioned Bulk Density} = \frac{\text{Split Mass after Conditioning}}{\text{Sample Volume}}$$

Figure 4.12 Schematic of conditioned bulk density measurement

Source: <http://www.freemantech.co.uk>

4.4.3.6 Compressibility. The measurement of Compressibility is achieved by applying increasing levels of compressive force with a piston to a conditioned powder and measuring the change in volume as a function of the applied load. The Vented Piston ensures that air trapped within the powder is able to readily escape, and the high resolution of the position measurement system allows for precise definition of Compressibility, expressed as a percentage change in volume for a given applied normal stress.

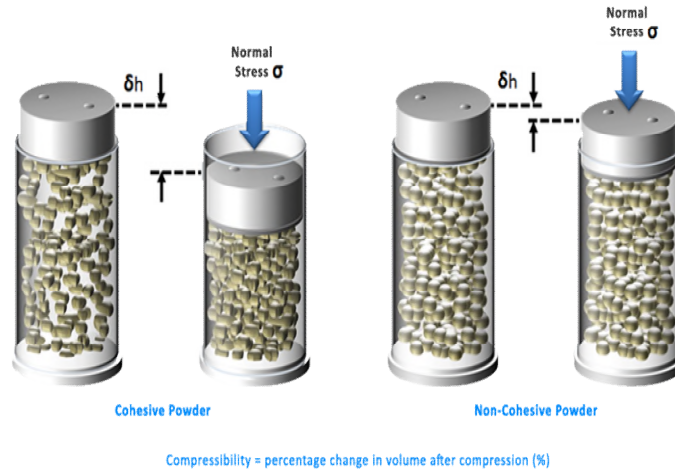


Figure 4.13 Schematic of Compressibility Test.

Source: <http://www.freemantech.co.uk>

Alternatively this data can be represented as a Compressibility Index or as Bulk Density, both as a function of applied normal stress.

4.4.3.7 Permeability. Permeability is a measure of the powder's resistance to air flow. Not to be confused with an Aeration test, this method utilizes the vented piston to constrain the powder column under a range of applied normal stresses, whilst air is passed through the powder column. The relative difference in air pressure between the bottom and the top of the powder column is a function of the powder's permeability. Tests can be completed under a range of normal stresses and air flow rates.

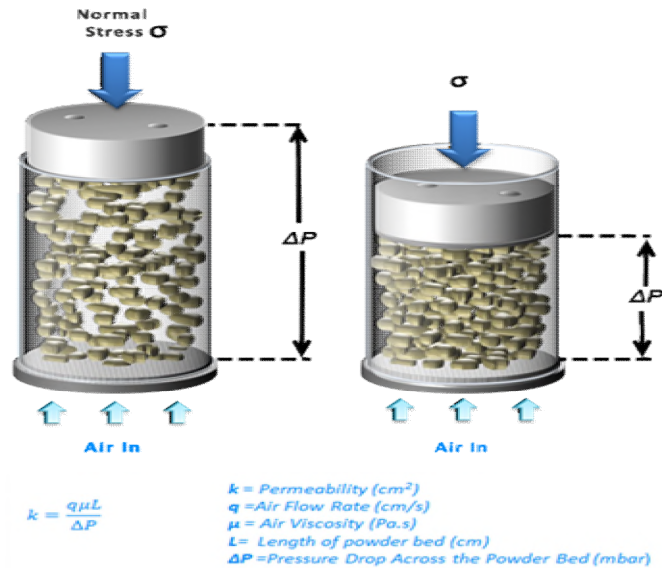


Figure 4.14 Schematic of Permeability Test.

Source: <http://www.freemantech.co.uk>

This important material property is relevant in many applications, including tableting and filling, for example. In a tableting process, the efficiency of air removal during the compression step will influence the mechanical properties of the compact, and should air be retained within the tablet due to low powder permeability, capping or lamination may occur. Within a filling application, the ability of the air to “back flow” out of the die or container through the powder as it enters depends on the bulk permeability and this will influence fill rate and fill consistency. Whilst permeability is a relatively simple bulk property, it is important in many processes and applications and should be accurately measured.

4.4.4 Flodex

The Gardco powder flowability test instrument is used to quantitatively determine the flowability of powder in terms of the flowability index on a scale of 4-40. The basis for

this method is the powder's ability to fall freely through a hole in a plate. The diameter of the smallest hole through which the powder passes three times out of three is taken as the flowability index.



Figure 4.15 Flodex.
Source: www.gardco.com

CHAPTER 5

APPLICATION IN PHARMACEUTICAL INDUSTRY

5.1 Improvement in Flowability of Cohesive Powders

Particles with different physical properties have very distinct flow behavior depending on the size, shape, material and surface properties. Geldart, (1973) based on empirical observations, was the first to classify the behavior of powders fluidized by gases into four groups: A, B, C, and D, depending on their size and the density difference between the solid particles and the fluidizing gas as shown in Figure 5.1. The distinction between these groups is related to the different fluidization behavior observed for each type of powders. In general, Geldart group A powders exhibit dense phase expansion after minimum fluidization and before the beginning of bubbling. Gas bubbles appear at the minimum bubbling velocity. Geldart group B powders bubble at minimum fluidization velocity and show small bed expansion. Geldart group C powders are extremely difficult to fluidize individually and generally will form cracks, channels or even lift as a solid plug when exposed to the fluidizing gas. Free particle motion for group C powders is suppressed by the dominant influence of cohesion forces. Geldart group D powders can easily form stable spouting beds.

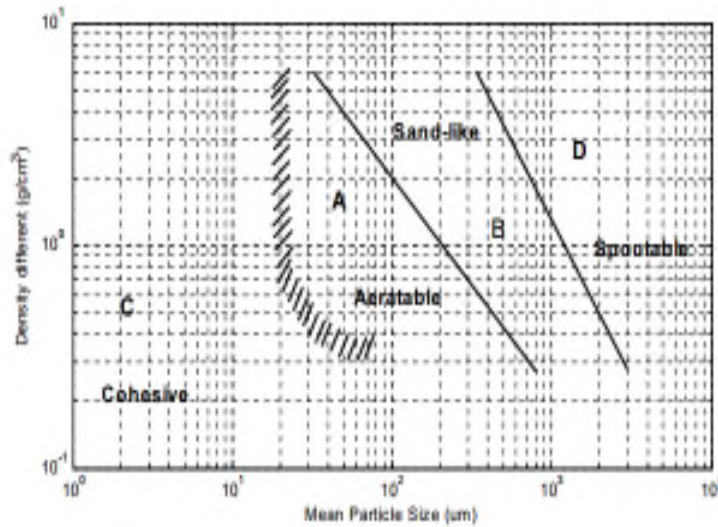


Figure 5.1 Geldart classification of powders.

Another effective criterion to classify the flowability of powders is the Bond number (Bo_g) which is defined as the ratio of inter-particle force to the force of gravity. It is clarified that the cohesiveness of the powder is negligible with $Bo_g < 1$ and the powder can be considered as free-flowing individually; otherwise, the powder is cohesive and tends to agglomerate. It has been found that the flowability of cohesive powders decreases when the granular Bond number $Bo_g = F_t / W$ increases using numerical simulation and experiments (Nase et al., 2001). Here, F_t is the inter-particle adhesion force and W is the particle weight.

The key issue is to improve the flow behavior of fine cohesive powders in various industries applications. However, how the Geldart law can be broken to improve the fluidization behavior of cohesive group C powders to that of the group A powders? The flowability of powders is determined by the Bond number. To enhance the flowability is to reduce the Bond number. Generally, there are two means to reduce the Bond number –

to reduce the interparticle cohesive force or to increase the gravitational force of particles. This is where dry coating comes into play. Dry coating reduces the inter-particle cohesive force by surface modification.

Yang and his co-workers showed an improvement in cornstarch coated with different grades of nano-sized silica using primarily the MAIC and Hybridizer. They have also used the V-blender and hand mixing for comparison purposes and concluded that these methods are less effective (Yang et al., 2005).

In 2006, Jiang evaluated flowability of composite particles prepared by coating PMMA with nano-particles TiO_2 , Al_2O_3 and SiO_2 using mechanofusion system and hand mixing by a vibratory capillary method. Analysis of surface morphology studies showed increased flowability and projected-area ratio of mechanofusion treated particles with increase in concentration of guest particles and was in the order of $\text{TiO}_2 > \text{Al}_2\text{O}_3 > \text{SiO}_2$. (Jiang et al., 2006).

In 2008, Chen and his co-workers used the dry coating technology to improve the flowability of Geldart Group C to Group A powders, by reducing the cohesiveness. They dry-coated corn starch and aluminium with various grades of nano-silica and studied the effect of SAC, i.e. the optimum amount of guest particle required to achieve good flowability(Chen et al., 2008).

In 2009, Ouabbas and his co-workers used the Cyclomix high shear granulator to dry coat silica gel particles with hydrophobic MgSt and starch with fumed silica. Flowability of the silica gel powder was significantly decreased after treatment the Cyclomix mixer with 15% of MgSt. It is also found that the coating by hydrophobic

MgSt in the Cyclomix can also reduce the high affinity between silica gel and water after treatment with 5% and 15% of MgSt.(Ouabbas et al., 2009b).

In 2010, Zhou used the mechanofusion system to improve the flowability of cohesive alpha lactose monohydrate by dry coating it with a traditional lubricant MgSt rather than a traditional glidant M5P(Zhou et al., 2010a).

In 2011, Chatteraj et al used the comil as the dry coating device to dry coat cellulose powder with colloidal silica to improve the flowability (Chatteraj et al., 2011).In the same year, Xi Han and her colleagues used the FEM to simultaneously micronize and dry coat Ibuprofen 110 with amorphous hydrophilic silica and studied the improvement in flowability(Han et al., 2011).

In 2012, Jallo et al used the MAIC to dry coat several APIs Ibuprofen 110, Ibuprofen 90, Ibuprofen 50, coarse and fine acetaminophen, crystalline and ultrafine ascorbic acid with hydrophobic and hydrophilic silica. They studied the improvement in flowability of the powders(Jallo et al., 2012).

In 2013, Zhou dry coated a pharmaceutical blend containing 75% ibuprofen, 22% microcrystalline cellulose (Avicel PH102), 3% sodium croscarmellose with colloidal silica M5P in a comil in order to improve the flowability and consequently manufacturability of the tablet(Zhou et al., 2013b).

In 2015, Huang and her colleagues used the comil as a continuous dry coating device to improve the flowability of a group of APIs coated with hydrophobic and hydrophilic silica(Huang et al., 2015).

5.2 Application in DPI Technology

The aerodynamic particle size of the micronized API in dry powder inhaler systems is 1 to 5 μm in order to be absorbed in the pulmonary tract. Such particles of very low sizes have a tendency to stick together via cohesive forces or to any other surface they encounter via adhesive forces, due to their high surface energy. These particles also exhibit very low aerosolization performance and poor flowability. Hence, in order to improve the flowability and aerosolization formulations of an API and a flow-aid is generally done.(Healy et al., 2014).

The most commonly used excipient in all DPI formulations is lactose monohydrate. A typical drug to carrier ratio is 1:67.5. (Larhrib et al., 1999). During inhalation, the APIs detach from the carrier and is deposited in the lungs. The larger carrier particles impact the mouth and are swallowed. The carrier provides bulk to the formulation which improves the handling, metering and flowability of the drug.

Mechanical dry coating using the theta-composer was used by Kawashima and his co-workers to dry coat micronized pranlukast hydrate, a selective active leukotriene antagonist for bronchial asthma with anhydrous silicic acid. This improvement in aerolization behavior was attributed to the surface modification of pranlukast, which decreased the cohesive forces between the particles.(Kawashima et al., 1998a).

In 2003, Iida and his group showed that the in vitro inhalation properties of salbutamol sulphate increased significantly on dry coating it with lactose using a theta-composer. The respiratory particle percent (RP) values were significantly increased on increasing the percentage of sucrose tristearate(Iida et al., 2003b). They followed it up in 2004 in a paper which showed inhalation properties were also improved by the surface

processing of lactose without any additive with decreased surface roughness and specific surface area (Sw)(Iida et al., 2004b). In another paper, they studied the effect of relative humidity on the in vitro inhalation property of salbutamol sulphate. They covered salbutamol sulphate with lactose coated with magnesium stearate by theta-composer. Coating of lactose with magnesium stearate showed increased humidity resistance which was due to increase in contact angle and hydrophobicity of lactose.(Iida et al., 2004a).

In 2005, Begat and his co-workers suggested the use of force control agents (leucine, lecithin and magnesium stearate) to condition the drug salbutamol sulphate rather than the carrier lactose to reduce cohesion and achieve improved DPI performance.(Begat et al., 2005).

In 2006, Kumon and his co-workers revealed that conditioning lactose with magnesium stearate or sucrose stearate in mechanofusion leads to greater fine particle fraction and improved DPI performance. They used the IGC to study the process(Kumon et al., 2006).They followed it up in 2008, where they proposed a mechanism of fine particle fraction formation with mechanofused magnesium stearate(Kumon et al., 2008a). In 2010, Zhou and his co-workers investigated the effect of coating magnesium stearate via the mechanofusion process to 3 model APIs salbutamol sulphate, salmeterol xinafoate, triamcinolone acetonide with different physical and chemical properties, on the aerosolization behavior. They found that the aerosolization significantly improves on dry coating(Zhou et al., 2010b). In 2013, they published another paper on dry coating salbutamol sulphate with magnesium stearate and studied the effect on aerosolization and DPI performance. They concluded that optimum performance was achieved at 2 wt. % MgSt.(Zhou et al., 2013c).

In 2012, another group of researchers studied the effect of different grades of lactose namely Flowlac® 100 (FLO), Lactopress anhydrous® 250 (LAC), Cellactose® 80 (CEL), Tablettose® 80 (TAB), and Granulac® 200 (GRA) which were blended with salbutamol sulphate in the ratio 1:67.5 and studied the DPI performance. They concluded that in vitro aerosolization for various lactose grades followed the following rank order in terms of deposition performance: GRA > TAB > LAC ≈ CEL > FLO (Kaialy et al., 2012).

5.3 Modification of Dissolution Profiles

5.3.1 Enhanced Dissolution

Dry coating leads to formation of composite particles with modified properties and one such application is the modification of dissolution characteristics.

In 1988, Ishizaka and his co-workers reported improved dissolution of aspirin on complexation with potato starch in a mechano-mill. They showed that although 90% of the powder dissolved in 5 minutes, more than 90% of the complex dissolved in 30s.(Ishizaka et al., 1988b). Later, in 1993, they showed the improved dissolution rates of indomethacin powder complexed with potato starch in hybridizer(ISHIZAKA et al., 1993).

In 2011, Han et al. studied the dissolution rates of ibuprofen micronized and dry coated with silica in a fluid energy mill. They concluded that the dry coated powder showed enhanced dissolution compared to the uncoated one (Han et al., 2011).

In 2012, Tay et al. studied the dissolution characteristics of a poorly water soluble drug indomethacin mechanofused with magnesium stearate (0.25%, 1%, and 5%) and sodium stearate (5%) and reported improvement(Tay et al., 2012).

5.3.2 Controlled Release

There are many papers in literature where plasticizer-dry-polymer coating has been utilized for controlled release of certain APIs.(Cerea et al., 2004; Pearnchob and Bodmeier, 2003a, b; Smikalla et al., 2011)

However, mechanical dry polymer coating papers are relatively few(Young et al., 2012; Zhang et al., 2010).

Capece et al. used the novel concept of mechanical dry coating of polymer to dry coat polyethylene wax onto ascorbic acid with the means of a vibratory mixer with steel balls. Dry coated ascorbic acid displayed delayed release profiles(Capece and Davé, 2014).They followed it up in 2015, with another paper which illustrates the mechanism of dry polymer coating where delayed release profiles of ascorbic acid and ibuprofen coated with polyethylene wax and carnauba wax were studied(Capece et al., 2015).

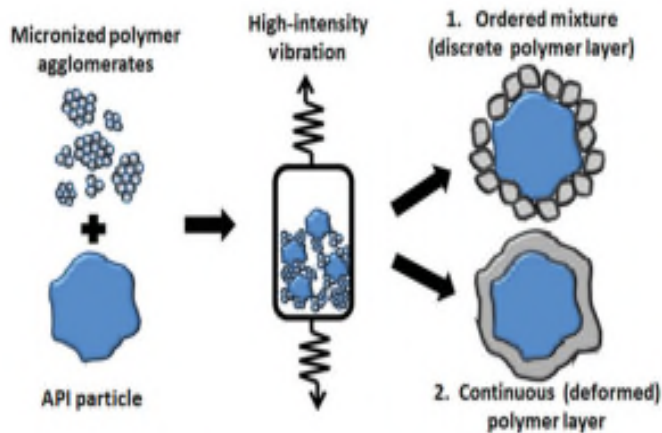


Figure 5.2 Graphic illustration of dry polymer coating process.
Source: (Capece et al., 2015)

CHAPTER 6

APPLICATION OF DRY COATING IN OTHER INDUSTRIES

6.1 Metal Composites

In 2003, Kim and his co-workers used the mechanical dry coating process to coat polymeric wax into copper for oxidation resistance, using the conventional ball mill(Kim et al., 2003).

In 2009, Yoshida et al, dry coated titania into alumina balls by mechanical coating and oxidation process and studied its photocatalytic activity(Yoshida et al., 2009).

In 2010, Laila et al. used the MAIC to dry coat aluminium particles with nano-sized silica, titania and carbon black to improve its flowability and cohesiveness. Aluminium is used as an additive in various energetic materials due to its high combustible nature.(Jallo et al., 2010).In the same year, Chen and his co-workers tried to characterize how surface coating with silica and silanization improves the flowability of cohesive aluminium powders(Chen et al., 2010a).

In 2012, Hao et al, used the traditional ball milling to coat zinc particles onto alumina in order to modify the properties of alumina(Hao et al., 2012).

6.2 Chromatographic Applications

In high performance liquid chromatography (HPLC) to obtain good results, it is imperative that the packing is uniform and regular shaped particles in the size range of 3-

10 μ m in diameter(Brown and Hartwick, 1988). Generally, silica gel particles or organic polymers with their surface modified with ion-exchange resins are used as packing material.

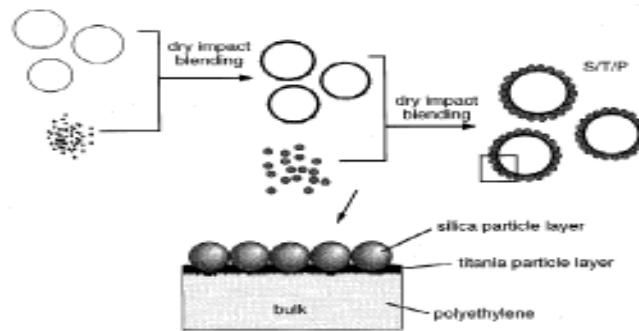


Figure 6.1 Schematic of double layer composite particles
Source: Honda 1997.

6.3 Refractory Materials – Sintering Applications

Deactivated sintering has been studied in the pioneering paper from our group(Mohan et al., 2003b).The phenomenon is called deactivated sintering because on increasing the sintering temperature the sintering rate decreases. They dry coated several host materials such as glass beads, polymethyl methacrylate (PMMA), γ -alumina, and an aluminium-silica composite with submicron sized silicon carbide in MAIC, mechanofusion and hybridizer. The discrete surface coating of silicon carbide on the alumina particles provided a deactivated layer which caused a significant reduction in the effective diffusivity of the coated material, resulting in a delay in the sintering of the material and an increase in then minimum sintering temperature. For amorphous materials, (glass and polymers) the deactivated layer of silicon carbide on the surface of glass beads and

PMMA caused an increase in the effective viscosity of the material retarding the flow of the softened PMMA or glass, resulting a delay in the sintering of the materials.

In the same year, Japanese group of researchers studied the sintering behavior of composites WC-Co/TiC-Al₂O₃ prepared by the hybridizer and sintered by the spark plasma method (SPS) and hot press. They concluded that the higher the rotational speed of the hybridizer, better is the mechanical properties and sintering temperature of the composites.(Kangwantrakool and Shinohara, 2003).

6.4 Food and Agriculture

In 2000, Watano and his co-workers used the theta composer to dry coat food fibre with hydrophilic silica. Food fibres are generally made out of cellulose and glucose and added to food for good digestive health. However, they are typically hygroscopic and this water retention property makes storage and preservation difficult. Hence the need for surface modification arose to suppress the hygroscopic properties of the food fibre. In the paper, they used Litesse III made of sorbitol and glucose as the host and hydrophilic silica as the guest. Dehydration reaction is expected to take place between the silanol groups of silica and the hydroxyl groups of food fibre leading to change in the hygroscopic nature, as illustrated in Figure 6.2(Watano et al., 2000).

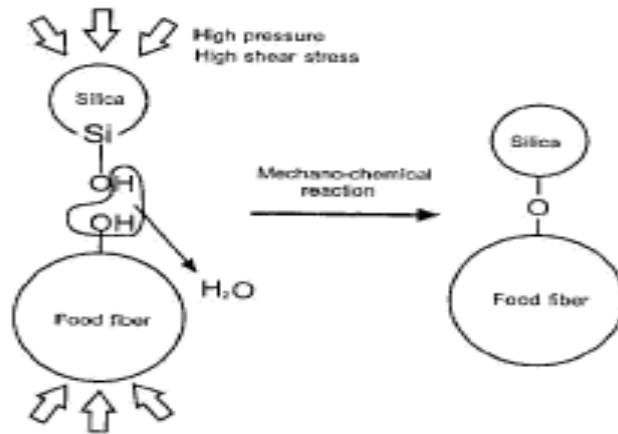


Figure 6.2 Schematic illustration of dehydration of food fibre mechano-chemically.
Source: Watano 2000.

In 2013, Narayanan and her co-workers published a review on the application of engineered composites in the food and agriculture sector. It reports the use of biosensors (dye-doped silica, quantum-dots, gold nano-particles) for protection against pesticides, nano-composites such as nano-clays and nano fibres and nano tubes in food packaging, nano-encapsulations and nano-emulsions in food processing (Narayanan et al., 2013).

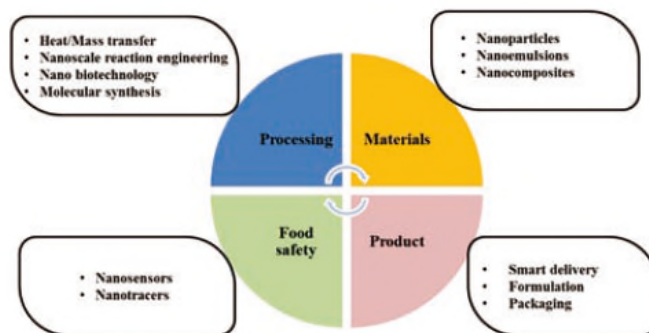


Figure 6.3 Application of nano-technology in food sector.
Source: Narayanan 2013.

6.5 Automobile Industry – Automotive catalysts

In order to meet the strict government regulations with regards to clean auto emissions, automotive catalysts have been used to reduce the emissions. Automotive catalysts generally consist of noble metals and potential transition metal oxides supported on alumina. The higher the surface area per unit volume of the catalyst, the less catalyst is required to achieve desired catalytic reaction efficiency, leading to a converter with smaller mass and volume. Therefore, nano catalysts have played an important role in the automobile industry. One of the newest techniques to manufacture nano-catalysts is to use the mechanical dry coating process.

In 2003, Coowanitwong and his co-workers used the theta composer to manufacture an alumina composite where γ -Al₂O₃ nano-particles were coated on Al₂O₃ fibre. The Al₂O₃ nanoparticles are well suited due to their high heat resistant properties and high surface area. Despite its low surface area, Al₂O₃ fiber has been selected for high temperature applications where space is at a premium due to its lightweight, low thermal conductivity and high stability. Incorporation of Al₂O₃ nanoparticles and Al₂O₃ fiber can therefore potentially yield lightweight composites with superior surface area and stability at high temperatures highly suitable for automotive catalyst applications (Coowanitwong et al., 2003).

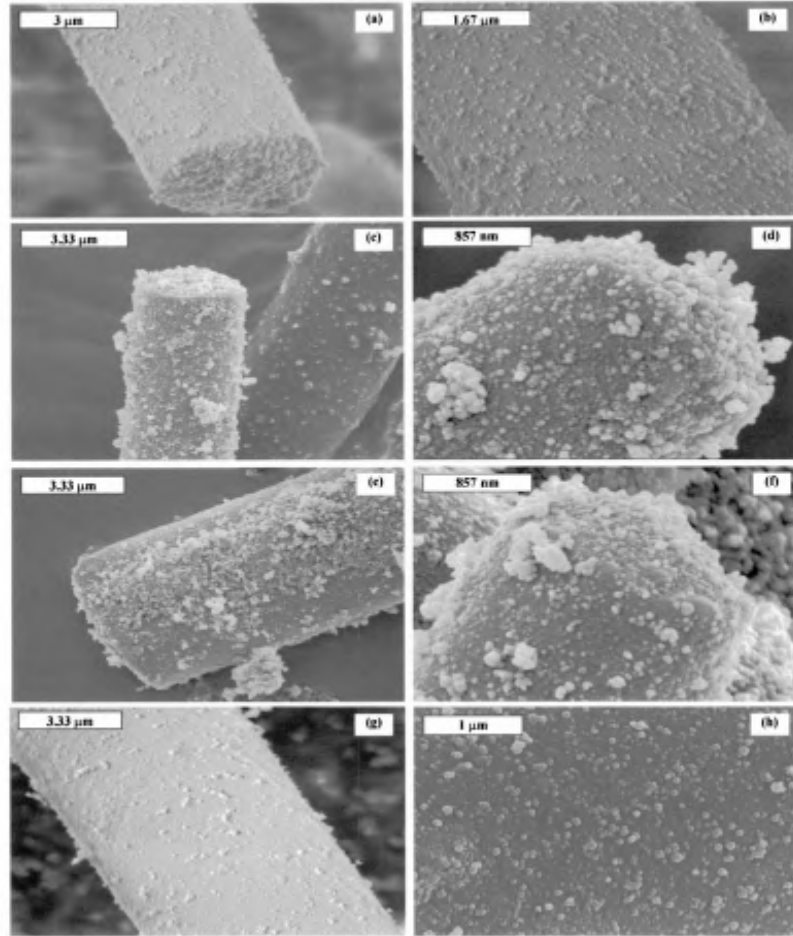


Figure 6.4 SEM Images of alumina nano-particles coated on alumina fibre.
Source: (Coowanitwong et al., 2003)

6.6 Thermal Insulation

The demand for good thermal insulation is growing worldwide, due to the ever increasing energy costs. Fumed silica compact boards have been established as an efficient insulator. Ceramic fibres are added to increase the cohesive nature of the board. However, fumed silica is very fragile and has to be handled with care, hence the number of fibres should be increased. However, increased fibres would result in higher heat transport.

In 2000, researchers proposed an alternative route to synthesize smarter insulation, as shown in Figure 6.5. Silica nanoparticles porously coated glass fiber composites are made at first stage and then they are compacted into a board. The composites are produced by a mechanical treatment of fumed silica and the fibers without collapse of the fumed silica's nanoscale pores. This is based on the fact that appropriate mechanical treatments of metal oxide powders can produce core/shell type composite particles without any binders in dry phase. The fumed silica-coating layer can prevent fiber–fiber direct contacts in the compact, which enables us to decrease solid thermal transport even at high solid loading of the fibers. The compact with relatively large amount of glass fibers (25 mass %) showed the excellent thermal insulation and sufficient strength for handling and machining(Abe et al., 2005).

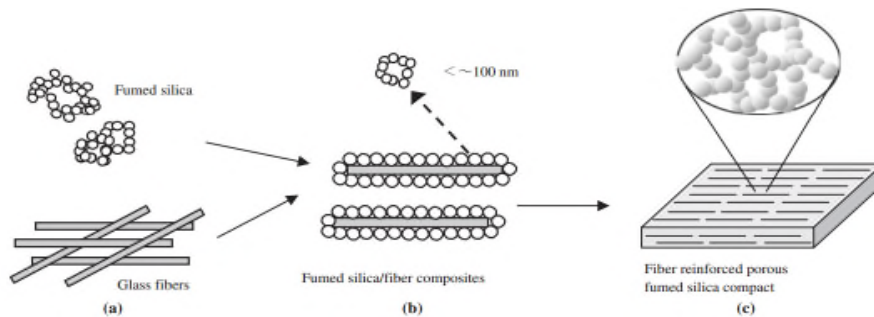


Figure 6.5: Schematic diagram of glass fibre reinforced fumed silica.

Source: (Abe et al., 2005)

6.7 Cosmetic Industry

In 1992, Nakane et al. reported several formulations of magnesium aluminometasilicate coated composite powders prepared by mechanofusion and hybridization system for the treatment of skin, deodorant and oral hygiene(Nakane et al., 1992).

Pongamia extract and soft shade DH (Powerful sparingly soluble UV light absorbers) are difficult to process in cosmetic formulations due to poor solubility in base agents. These agents were coated on sericite powder by mechanofusion and subsequently used in formulation of solid foundations, sunscreen products and white powder with superior ultraviolet light protection effect and stability overtime (Ogawa et al., 2000).

Lipophilic base powders were covered with zinc oxide powder by mechanofusion and dispersed in oily phase with some additives like sequestering agents, whitening agents and drugs. Base powder adsorbed plasminogen activator and zinc ions eluted from zinc and contributed to rough skin recovering/preventing effect. Appearance of skin also improved due to improvement in skin color, non-uniformity hiding effect and irregularity shading off the effect (Suda et al., 2006).

Lefebvre et al., studied the wettability and dispersibility of talc – a powder important in cosmetic, paints and pharmaceuticals. They dry coated talc ($\text{Mg}_3\text{Si}_4\text{O}_{10}(\text{OH})_2$), with hydrophobic R972P silica using a cyclomix high shear mixer. The SEM micrographs of talc and silica are shown in Figure 6.6 (Lefebvre et al., 2011).

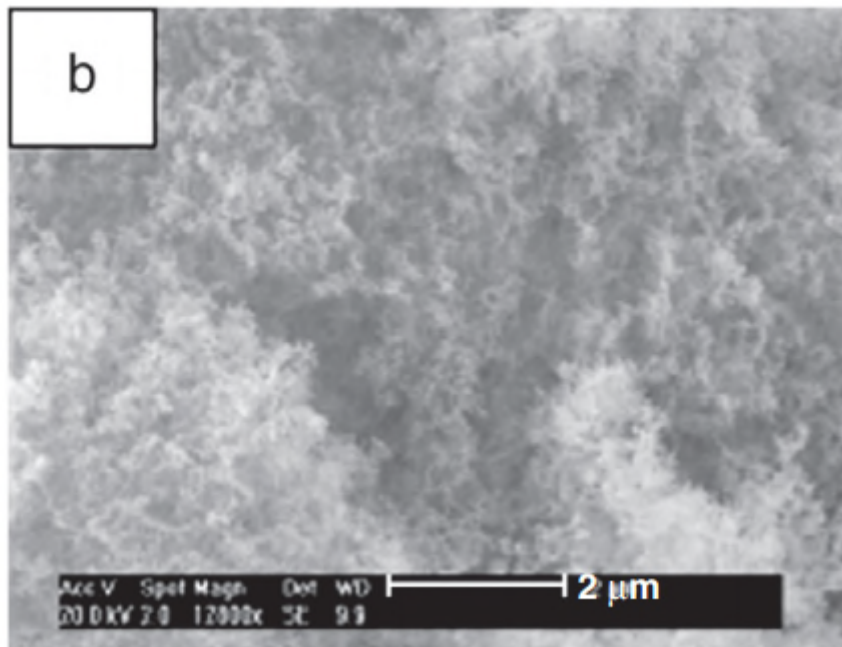
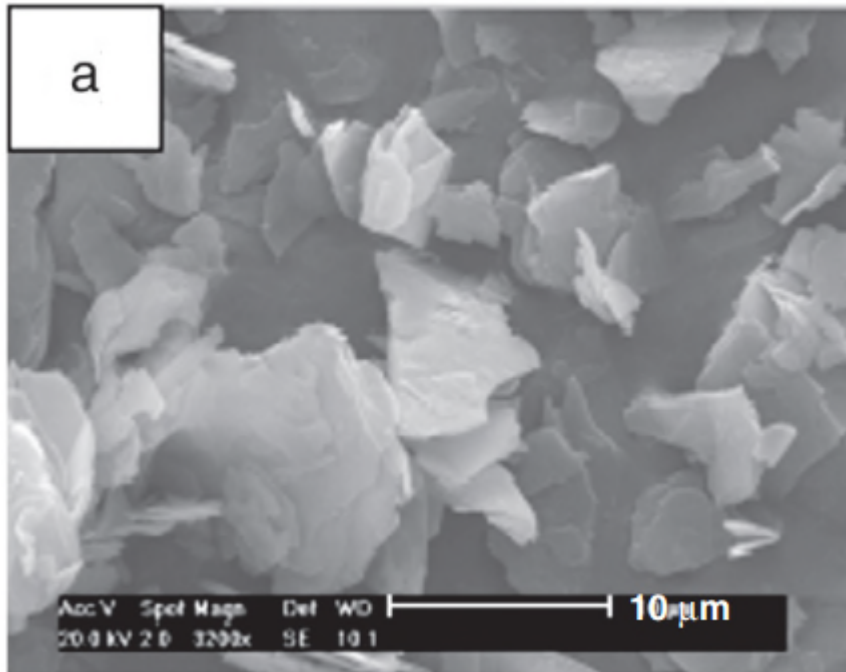


Figure 6.6 (a) Talc particles ($\times 3200$) and (b) Aerosil R972[®] particles ($\times 12,600$).
Source:(Lefebvre et al., 2011)

6.8 Lithium Ion Batteries

With the increase in demand of consumer electronic goods, like computers and other communication devices, the need for batteries with higher capacities is on the rise.

In 2008, Chou and his co-workers used the mechanofusion system to form a composite particle consisting of nano-ferric oxide and nano-nickel oxide on the surface of artificial mesophase graphite powder (MGP) to replace the carbon anode of the lithium ion battery. Figure 6.7 shows the schematic of the lithium ion battery. The use of MGP/nano-Fe₂O₃ composite particles as the carbon anode material of lithium ion semi-batteries substantially reduces the irreversible capacity. Most importantly, this study supports the application of the MGP/nano-Fe₂O₃ composite particles to improve the performance of lithium ion semi-batteries.(Chou et al., 2008)

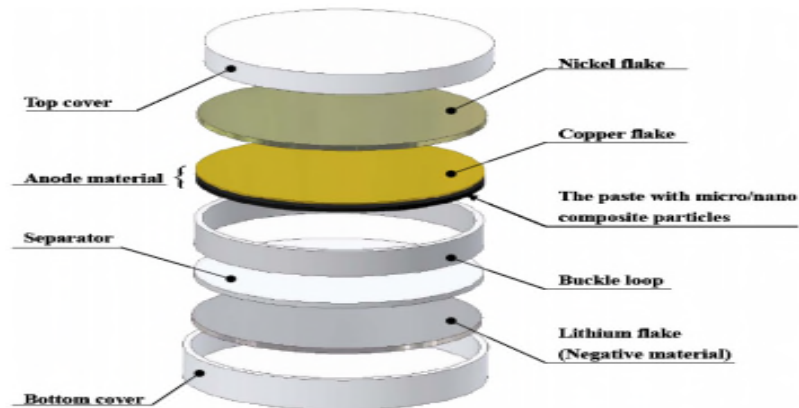


Figure 6.7 Schematic of lithium ion battery.

Source:(Chou et al., 2008)

6.9 Paints and Paper

Titanium dioxide (TiO₂) is the most widely-used white pigment in industry with good pigment properties such as strong hiding power, good dispersity and excellent weather

resistance, etc. However, due to environmental pollution and high resource consumption, the production of titanium oxide is hampered. In order to overcome this problem, Deng et al, in 2008, prepared a composite particle with titanium oxide as the shell and calcined kaolin (a mineral) as the outer layer using the mechanofusion system. They evaluated the characteristics of the composite and concluded that it has excellent pigment properties(Deng, 2010).

In 2015, Cho and Lee (Cho and Lee, 2015) prepared composite materials with pigments and minerals usually used for paper-making. They also used titanium dioxide as the pigment and dry coated it with ground calcium carbonate, clay and talc in the mechanofusion system. Figure 6.7 shows the SEM images of GCC (a) and titanium dioxide modified GCC (b). They measured a number of optical and electrostatic properties and the results of zeta potential is shown in Figure 6.9. They concluded that the surface modification of the pigments were ascertained by their properties and their results will help in paper-making. (Cho and Lee, 2015).

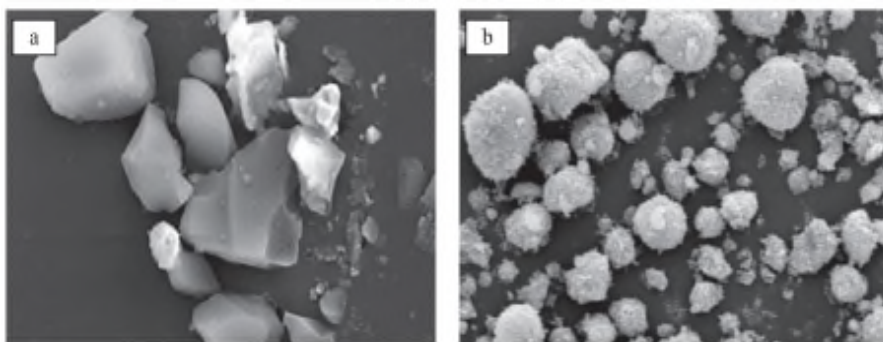


Figure 6.8 SEM images of GCC pigment (a) and GCC pigment modified with titanium oxide (b).

Source: (Cho and Lee, 2015)

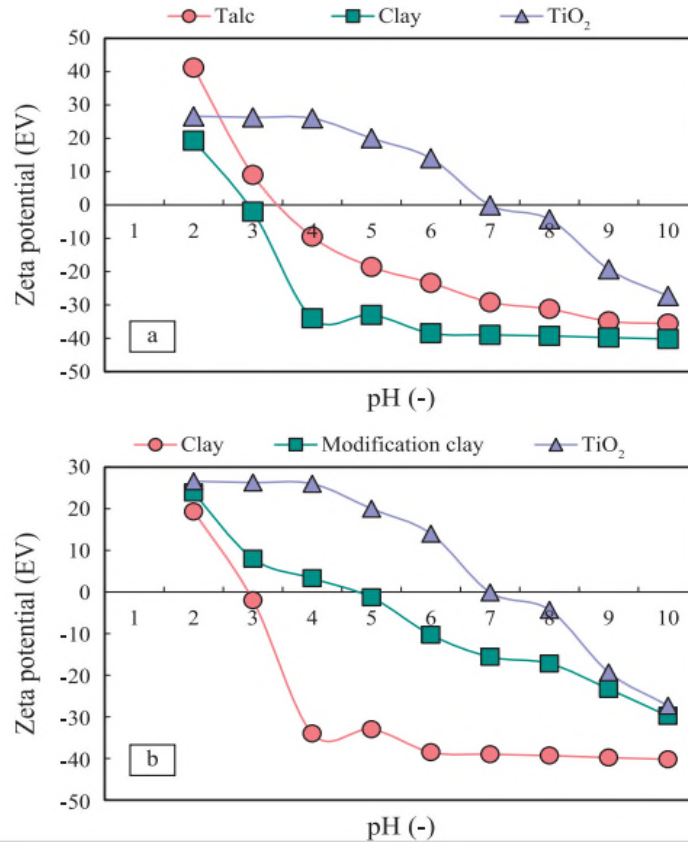


Figure 6.9 Zeta potential (a) non-modified pigments (b) clay modified pigments.
Source : (Cho and Lee, 2015)

6.10 Miscellaneous Applications

At NJIT, several composite particles are prepared with the help of any one or more of the dry coating equipment to serve various functionalities. Some of them are given below.

6.10.1 Nano Silica Coating of Silica, Aluminum Nitride and Boron Nitride Host Particles

The objectives of coating nano-sized silica onto aluminum nitride and boron nitride are:

- (1) to increase the filler loading capability to increase thermal conductivity;
- (2) to stabilize the fillers surface and
- (3) to increase the thixo index. The purpose of coating

nano-silica onto micron sized silica is to complete the rheology work done on the silica coated aluminum nitride system and to see whether the temperature dependency is based on the core material or the coating process. The coating experiments are carried out by using MAIC and HB for AlN and BN, but only the MAIC is used for silica coating.

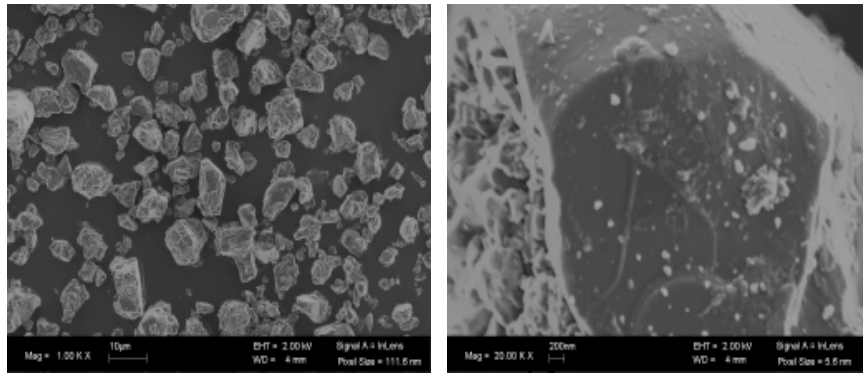


Figure 6.10 SEM images of AlN as received.

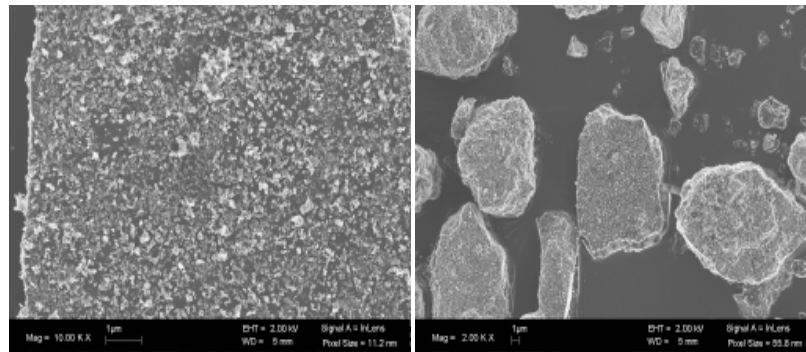


Figure 6.11 AlN coated with 2.0% R972 by MAIC (10 minutes).

6.10.2 Coating of ITO onto ATO/Mica

The objective of coating ITO onto Mica is to develop filler that will have ITO conductive properties, and lower cost than 100% ITO filled material. The coating experiments are carried out using MAIC and HB, and in some cases, MAIC is followed by HB for the same batch of product.

6.10.3 Carbon Coating of Copper for Conductivity and Oxidation Control

The objective of coating carbon onto copper is to reduce the surface oxidation. The coating experiments were conducted by MAIC. The coating experiments are carried out by using MAIC.

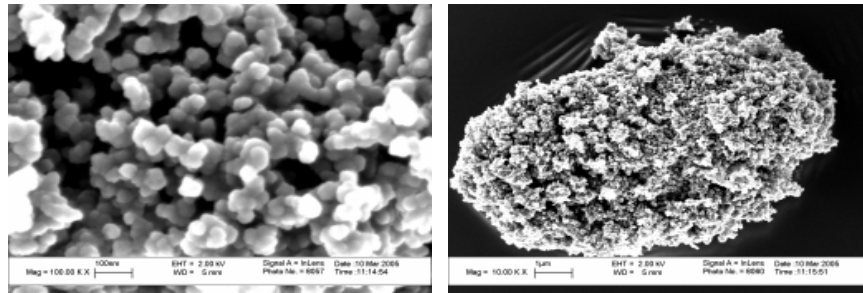


Figure 6.12 Carbon black XE2 (As received).

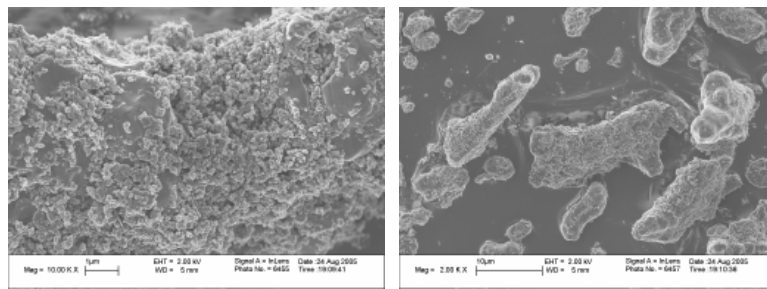


Figure 6.13 UCF5 CBXE2 1% MAIC coating.

6.10.4 Coating of Silver onto Copper for Improved Conductivity

The purpose is to develop a filler system with high conductivity at low cost. Copper may also prevent silver migration. The coating experiments are carried out by using MAIC.

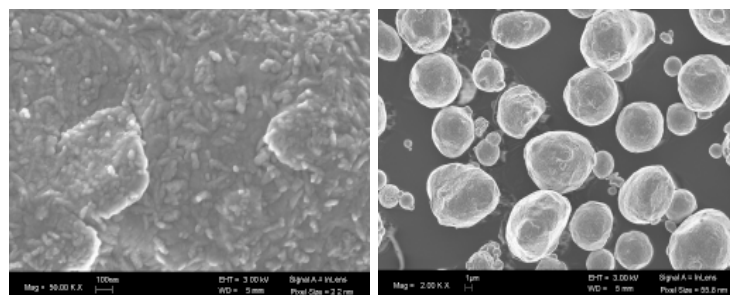


Figure 6.14 Copper (As received).

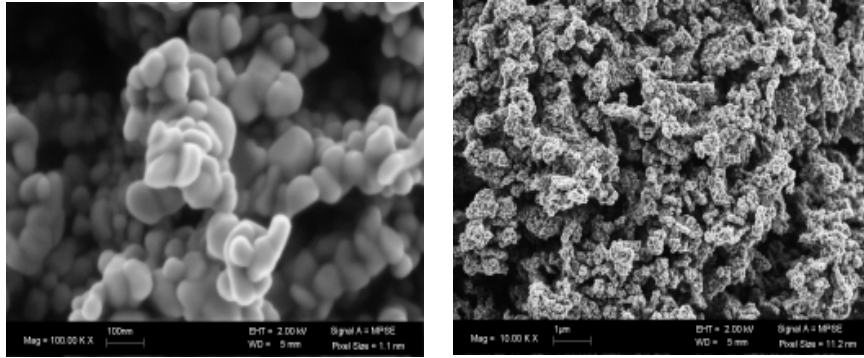


Figure 6.15 30 nm Ag (As received).

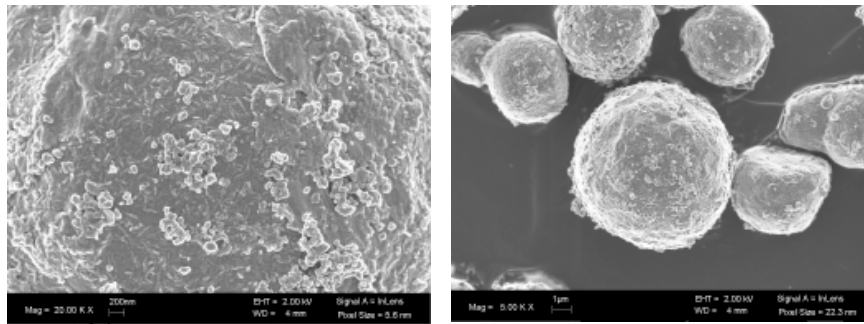


Figure 6.16 30nm Ag-10 Cu-HB-6000rpm-5 mins-2.8%.

6.10.5 Coating of Nano-sized Copper Oxide onto Silver Flakes for Improved Adhesion

The purpose is to add CuO coating onto silver flakes to increase adhesion, reduce voiding of CuO, increase moisture resistance test (MRT) for E & C.

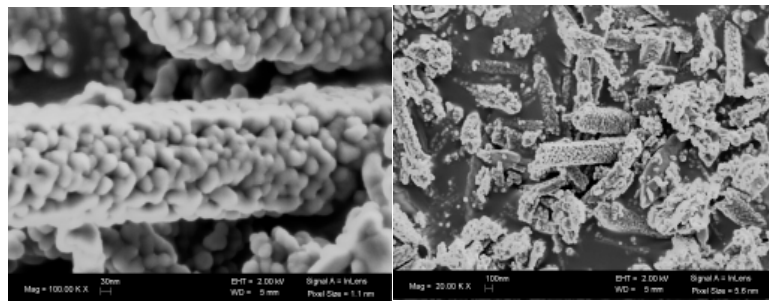


Figure 6.17 Nano-sized copper (II) oxide.

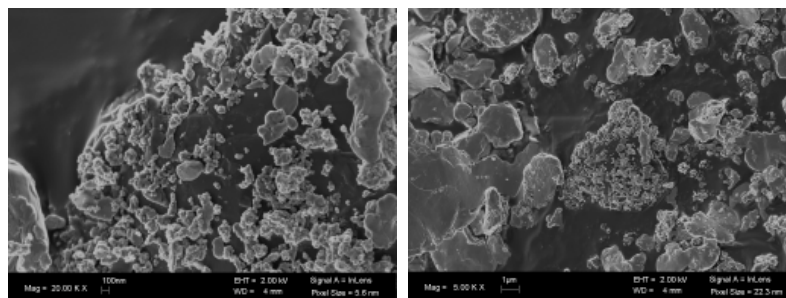


Figure 6.18 CuO-Silver flakes -MAIC (5%).

6.10.6 Catalyst Encapsulation by dry particle coating

The purpose is to create a protective coating layer onto the catalyst surface to extend its shelf life. Three kinds of catalyst Ancamine 2337, Anca 2014FG and Cure201c17z were coated with A200 or R972 respectively.

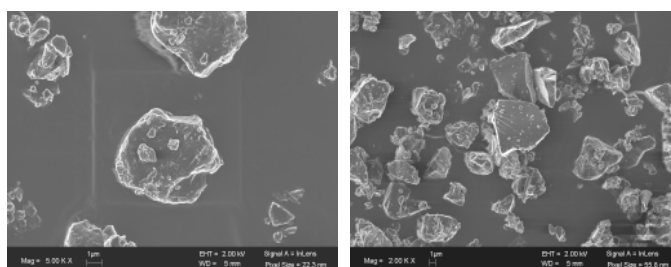


Figure 6.19 Ancamine 2337 (As Received).

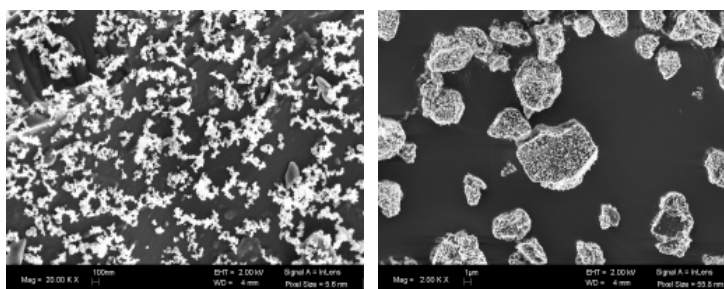


Figure 6.20 Ancamine 2337 coated with 5% of R972 by MAIC for 15 mins.

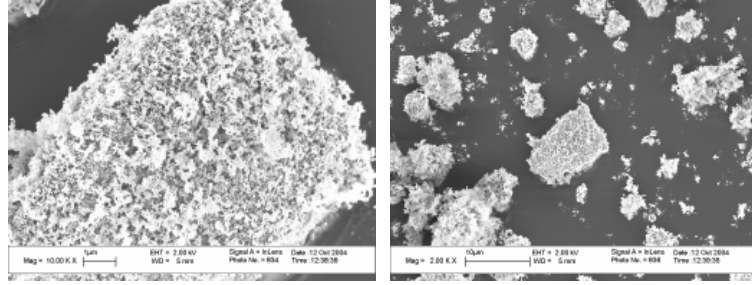


Figure 6.21 Anca2014FG coated with 50% of R972 by MAIC for 15 mins.

CHAPTER 7

CONCLUSIONS

In this thesis work, an attempt has been made to review the literature of dry coating experiments from the early years to the latest development. Several theories have been proposed to explain the mechanism of dry coating. There are also various devices which are used for dry coating. The current state-of –the-art approach is to optimize each device according to the requirement. The characterization methods which are most commonly used are described in brief. Finally, the various applications of this technology is given in a chronological order.

It is hoped that this review will serve as an excellent source of information for current and future researchers and serve to open up newer frontiers in dry particle coating technology.

REFERENCES

- Abe, H., Abe, I., Sato, K., Naito, M., 2005. Dry powder processing of fibrous fumed silica compacts for thermal insulation. *Journal of the American Ceramic Society* 88, 1359-1361.
- Alonso, M., Satoh, M., Miyanami, K., 1988. Powder coating in a rotary mixer with rocking motion. *Powder technology* 56, 135-141.
- Alonso, M., Satoh, M., Miyanami, K., 1989. Mechanism of the combined coating-mechanofusion processing of powders. *Powder Technology* 59, 45-52.
- Alvarez, R.C., Ageorges, H., Fauchais, P., 2003. Alumina reinforced stainless steel coatings by plasma spraying mechanofused particles, *International Surface Engineering Congress - Proceedings of the 1st Congress*, pp. 544-548.
- Beach, L., Roper, J., Mujumdar, A., Alcalà, M., Romañach, R.J., Davé, R.N., 2010. Near-infrared spectroscopy for the in-line characterization of powder voiding part II: Quantification of enhanced flow properties of surface modified active pharmaceutical ingredients. *Journal of Pharmaceutical Innovation* 5, 1-13.
- Begat, P., Morton, D.A.V., Shur, J., Kippax, P., Staniforth, J.N., Price, R., 2009. The role of force control agents in high-dose dry powder inhaler formulations. *Journal of Pharmaceutical Sciences* 98, 2770-2783.
- Begat, P., Price, R., Harris, H., Morton, D.A., Staniforth, J.N., 2005. The influence of force control agents on the cohesive-adhesive balance in dry powder inhaler formulations. *Kona* 23, 109-121.
- Bowling, R., Mittal, K., 1988. *Particles on Surfaces 1: Detection, Adhesion, and Removal*. KL Mittal (Ed.) 2, 129.
- Brown, P., Hartwick, R.A., 1988. High performance liquid chromatography.
- Capece, M., Barrows, J., Davé, R.N., 2015. Controlled Release from Drug Microparticles via Solventless Dry-Polymer Coating. *Journal of pharmaceutical sciences*.
- Capece, M., Davé, R.N., 2014. Solventless polymer coating of microparticles. *Powder Technology* 261, 118-132.
- Capece, M., Huang, Z., To, D., Aloia, M., Muchira, C., Dave, R., Yu, A., 2014. Prediction of porosity from particle scale interactions: Surface modification of fine cohesive powders. *Powder Technology* 254, 103-113.
- Carr, R.L., 1965. Evaluating flow properties of solids. *Chem. Eng* 72, 163-168.
- Cerea, M., Zheng, W., Young, C.R., McGinity, J.W., 2004. A novel powder coating process for attaining taste masking and moisture protective films applied to tablets. *International journal of pharmaceuticals* 279, 127-139.

- Chattoraj, S., Shi, L., Sun, C.C., 2011. Profoundly improving flow properties of a cohesive cellulose powder by surface coating with nano-silica through comilling. *Journal of pharmaceutical sciences* 100, 4943-4952.
- Chen, Y., Jallo, L., Quintanilla, M.A., Dave, R., 2010a. Characterization of particle and bulk level cohesion reduction of surface modified fine aluminum powders. *Colloids and Surfaces A: Physicochemical and Engineering Aspects* 361, 66-80.
- Chen, Y., Jallo, L., Quintanilla, M.A.S., Dave, R., 2010b. Characterization of particle and bulk level cohesion reduction of surface modified fine aluminum powders. *Colloids and Surfaces A: Physicochemical and Engineering Aspects* 361, 66-80.
- Chen, Y., Yang, J., Dave, R.N., Pfeffer, R., 2008. Fluidization of coated group C powders. *AIChE Journal* 54, 104-121.
- Cho, J.H., Lee, Y.W., 2015. Preparation of Composite Powder and Properties by Surface Modification of Inorganic Pigments for Papermaking.
- Chou, C.-S., Tsou, C.-H., Wang, C.-I., 2008. Preparation of graphite/nano-powder composite particles and applicability as carbon anode material in a lithium ion battery. *Advanced Powder Technology* 19, 383-396.
- Cooper, D., Yasensky, D., Wu, C.Y., Butt, D., Cai, M., Ruskoski, M., Rogers, J., 2004. Evaluation of Ni-nanoparticle coated magnesium powder synthesized by dry mechanical process for hydrogen storage, *ACS National Meeting Book of Abstracts*, 1 ed, pp. IEC-170.
- Coowanitwong, N., Wu, C.-Y., Nguyen, J., Cai, M., Ruthkosky, M., Rogers, J., Feng, L., Watano, S., Yoshida, T., 2003. Surface enhancement of Al₂O₃ fiber with nanosized Al₂O₃ particles using a dry mechanical coating process. *Journal of engineering materials and technology* 125, 163-169.
- Deng, Y., 2010. Characterization of calcined kaolin/TiO₂ composite particle material prepared by mechano-chemical method. *Journal of Wuhan University of Technology-Mater. Sci. Ed.* 25, 765-769.
- Derjaguin, B.V., Muller, V.M., Toporov, Y.P., 1975. Effect of contact deformations on the adhesion of particles. *Journal of Colloid and interface science* 53, 314-326.
- Dutta, A., Dullea, L.V., 1990. Comparative evaluation of negatively and positively charged submicron particles as flow conditioners for a cohesive powder, *AIChE Symposium Series*, 276 ed, pp. 26-40.
- Fan, L., Chen, Y.-M., Lai, F., 1990. Recent developments in solids mixing. *Powder Technology* 61, 255-287.
- Farne, G., Genel Ricciardiello, F., Kucich Podda, L., Minichelli, D., 1997. Sintering of ZrO₂ - CeO₂ - Y₂O₃ alloys: Influence of powder preparation, *Key Engineering Materials*, pp. 876-879.
- Fukui, T., Murata, K., Ohara, S., Abe, H., Naito, M., Nogi, K., 2004. Morphology control of Ni-YSZ cermet anode for lower temperature operation of SOFCs. *Journal of Power Sources* 125, 17-21.

- Fukui, T., Ohara, S., Okawa, H., Naito, M., Nogi, K., 2003. Synthesis of metal and ceramic composite particles for fuel cell electrodes. *Journal of the European Ceramic Society* 23, 2835-2840.
- Fukui, T., Okawa, H., Hotta, T., Naito, M., Yokoyama, T., 2001. Synthesis of CoO/Ni Composite Powders for Molten Carbonate Fuel Cells. *Journal of the American Ceramic Society* 84, 233-235.
- Gera, M., Saharan, V.A., Kataria, M., Kukkar, V., 2010. Mechanical methods for dry particle coating processes and their applications in drug delivery and development. *Recent patents on drug delivery & formulation* 4, 58-81.
- Ghoroi, C., Gurumurthy, L., McDaniel, D.J., Jallo, L.J., Davé, R.N., 2013a. Multi-faceted characterization of pharmaceutical powders to discern the influence of surface modification. *Powder Technology* 236, 63-74.
- Ghoroi, C., Han, X., To, D., Jallo, L., Gurumurthy, L., Davé, R.N., 2013b. Dispersion of fine and ultrafine powders through surface modification and rapid expansion. *Chemical Engineering Science* 85, 11-24.
- Guerin, E., Tchoreloff, P., Leclerc, B., Tanguy, D., Deleuil, M., Couarraze, G., 1999. Rheological characterization of pharmaceutical powders using tap testing, shear cell and mercury porosimeter. *International Journal of Pharmaceutics* 189, 91-103.
- Han, X., Ghoroi, C., Davé, R., 2013a. Dry coating of micronized API powders for improved dissolution of directly compacted tablets with high drug loading. *International Journal of Pharmaceutics* 442, 74-85.
- Han, X., Ghoroi, C., To, D., Chen, Y., Davé, R., 2011. Simultaneous micronization and surface modification for improvement of flow and dissolution of drug particles. *International Journal of Pharmaceutics* 415, 185-195.
- Han, X., Jallo, L., To, D., Ghoroi, C., Davé, R., 2013b. Passivation of high-surface-energy sites of milled ibuprofen crystals via dry coating for reduced cohesion and improved flowability. *Journal of Pharmaceutical Sciences* 102, 2282-2296.
- Hao, L., Lu, Y., Sato, H., Asanuma, H., 2012. Fabrication of zinc coatings on alumina balls from zinc powder by mechanical coating technique and the process analysis. *Powder Technology* 228, 377-384.
- Harnby, N., 1967. A comparison of the performance of industrial solids mixers using segregating materials. *Powder technology* 1, 94-102.
- Hausner, H., 1967. FRICTION CONDITIONS IN A MASS OF METAL POWDER. Polytechnic Inst. of Brooklyn. Univ. of California, Los Angeles.
- Healy, A.M., Amaro, M.I., Paluch, K.J., Tajber, L., 2014. Dry powders for oral inhalation free of lactose carrier particles. *Advanced Drug Delivery Reviews* 75, 32-52.
- Hendrickson, W.A., Abbott, J., 1999. Utilizing magnetic forces to fluidize particulate material in the presence of liquids within forces to fluidize particulate material in the presence of liquids within the fluidized bed. Google Patents.

- Herman, H., Chen, Z.J., Huang, C.C., Cohen, R., 1992. Mechanofused powders for thermal spray. *Journal of Thermal Spray Technology* 1, 129-135.
- Hersey, J.A., 1975. Ordered mixing: a new concept in powder mixing practice. *Powder Technology* 11, 41-44.
- Hiestand, E., 1991. Tablet bond. I. A theoretical model. *International journal of pharmaceutics* 67, 217-229.
- Hiestand, E., Smith, D., 1991. Tablet bond. II. Experimental check of model. *International journal of pharmaceutics* 67, 231-246.
- Hoashi, Y., Tozuka, Y., Takeuchi, H., 2013. Solventless dry powder coating for sustained drug release using mechanochemical treatment based on the tri-component system of acetaminophen, carnauba wax and glidant. *Drug Development and Industrial Pharmacy* 39, 259-265.
- Hollenbach, A.M., Peleg, M., Rufner, R., 1983. Interparticle surface affinity and the bulk properties of conditioned powders. *Powder Technology* 35, 51-62.
- Huang, Z., Scicolone, J.V., Gurumuthy, L., Davé, R.N., 2015. Flow and bulk density enhancements of pharmaceutical powders using a conical screen mill: A continuous dry coating device. *Chemical Engineering Science* 125, 209-224.
- Iida, K., Hayakawa, Y., Okamoto, H., Danjo, K., Luenberger, H., 2003a. Effect of surface covering of lactose carrier particles on dry powder inhalation properties of salbutamol sulfate. *Chemical and Pharmaceutical Bulletin* 51, 1455-1457.
- Iida, K., Hayakawa, Y., Okamoto, H., Danjo, K., Luenberger, H., 2004a. Influence of storage humidity on the in vitro inhalation properties of salbutamol sulfate dry powder with surface covered lactose carrier. *Chemical and pharmaceutical bulletin* 52, 444-446.
- Iida, K., Hayakawa, Y., Okamoto, H., Danjo, K., Luenberger, H., 2003b. Effect of surface covering of lactose carrier particles on dry powder inhalation properties of salbutamol sulfate. *Chemical and pharmaceutical bulletin* 51, 1455-1457.
- Iida, K., Inagaki, Y., Todo, H., Okamoto, H., Danjo, K., Luenberger, H., 2004b. Effects of surface processing of lactose carrier particles on dry powder inhalation properties of salbutamol sulfate. *Chemical and pharmaceutical bulletin* 52, 938-942.
- Ishizaka, T., Honda, H., Ikawa, K., Kizu, N., Yano, K., Koishi, M., 1988a. Complexation of aspirin with potato starch and improvement of dissolution rate by dry mixing. *Chem. Pharm. Bull* 36, 2562-2569.
- Ishizaka, T., Honda, H., Ikawa, K., Kizu, N., Yano, K., Koishi, M., 1988b. Complexation of Aspirin with Potato Starch and Improvement of Dissolution Rate by Dry Mixing. *CHEMICAL & PHARMACEUTICAL BULLETIN* 36, 2562-2569.
- ISHIZAKA, T., HONDA, H., KOISHI, M., 1993. Drug Dissolution from Indomethacin-starch Hybrid Powders Prepared by the Dry Impact Blending Method. *Journal of pharmacy and pharmacology* 45, 770-774.

- Jallo, L.J., Ghoroi, C., Gurumurthy, L., Patel, U., Davé, R.N., 2012. Improvement of flow and bulk density of pharmaceutical powders using surface modification. *International Journal of Pharmaceutics* 423, 213-225.
- Jallo, L.J., Schoenitz, M., Dreizin, E.L., Dave, R.N., Johnson, C.E., 2010. The effect of surface modification of aluminum powder on its flowability, combustion and reactivity. *Powder Technology* 204, 63-70.
- Jay, F., Gauthier, V., Dubois, S., 2006. Iron particles coated with alumina: Synthesis by a mechanofusion process and study of the high-temperature oxidation resistance. *Journal of the American Ceramic Society* 89, 3522-3528.
- Jiang, Y., Matsusaka, S., Masuda, H., Yokoyama, T., 2006. Evaluation of flowability of composite particles and powder mixtures by a vibrating capillary method. *Journal of Chemical Engineering of Japan* 39, 14-21.
- Johnson, K., Kendall, K., Roberts, A., 1971. Surface energy and the contact of elastic solids, *Proceedings of the Royal Society of London A: Mathematical, Physical and Engineering Sciences*. The Royal Society, pp. 301-313.
- Kaga, H., Shiono, I., Taya, Y., Takamura, T., Sugawara, T., Katayama, H., 1990. Preparation of Cu/Al₂O₃ composite particles by vacuum mechanofusion process. *Funtai Oyobi Fumatsu Yakin/Journal of the Japan Society of Powder and Powder Metallurgy* 37, 995-1000.
- Kaialy, W., Ticehurst, M., Nokhodchi, A., 2012. Dry powder inhalers: Mechanistic evaluation of lactose formulations containing salbutamol sulphate. *International Journal of Pharmaceutics* 423, 184-194.
- Kangwantrakool, S., Shinohara, K., 2003. Sintering behavior of mechanically coated WC-Co/TiC-Al₂O₃ particles by high-speed rotational impact blending. *International Journal of Refractory Metals and Hard Materials* 21, 171-182.
- Kato, T., Ushijima, H., Katsumata, M., Hyodo, T., Shimizu, Y., Egashira, M., 2002. Fabrication of hollow alumina microspheres via core/shell structure of polymethylmethacrylate/alumina prepared by mechanofusion. *Journal of Materials Science* 37, 2317-2321.
- Kato, T., Ushijima, H., Katsumata, M., Hyodo, T., Shimizu, Y., Egashira, M., 2004. Effect of core materials on the formation of hollow alumina microspheres by mechanofusion process. *Journal of the American Ceramic Society* 87, 60-67.
- Kawashima, Y., Serigano, T., Hino, T., Yamamoto, H., Takeuchi, H., 1998a. Design of inhalation dry powder of pranlukast hydrate to improve dispersibility by the surface modification with light anhydrous silicic acid (AEROSIL 200). *International Journal of Pharmaceutics* 173, 243-251.
- Kawashima, Y., Serigano, T., Hino, T., Yamamoto, H., Takeuchi, H., 1998b. Design of inhalation dry powder of pranlukast hydrate to improve dispersibility by the surface modification with light anhydrous silicic acid (AEROSIL 200). *International Journal of Pharmaceutics* 173, 243-251.

- Kim, B.-K., Lee, J.-S., Lee, C.-H., Park, D.-J., 2008. Preparation of low-fat uptake frying batter composite by dry particle coating of microparticulated soybean hull. *LWT - Food Science and Technology* 41, 34-41.
- Kim, J., Satoh, M., Iwasaki, T., 2003. Mechanical-dry coating of wax onto copper powder by ball milling. *Materials Science and Engineering: A* 342, 258-263.
- Kumon, M., Machida, S., Suzuki, M., Kusai, A., Yonemochi, E., Terada, K., 2008a. Application and mechanism of inhalation profile improvement of DPI formulations by mechanofusion with magnesium stearate. *Chemical and Pharmaceutical Bulletin* 56, 617-625.
- Kumon, M., Suzuki, M., Kusai, A., Yonemochi, E., Terada, K., 2006. Novel approach to DPI carrier lactose with mechanofusion process with additives and evaluation by IGC. *Chemical and Pharmaceutical Bulletin* 54, 1508-1514.
- Kumon, M., Yabe, Y., Kasuya, Y., Suzuki, M., Kusai, A., Yonemochi, E., Terada, K., 2008b. Applicability of DPI formulations for novel neurokinin receptor antagonist. *International Journal of Pharmaceutics* 356, 102-109.
- Larhrib, H., Zeng, X.M., Martin, G.P., Marriott, C., Pritchard, J., 1999. The use of different grades of lactose as a carrier for aerosolised salbutamol sulphate. *International Journal of Pharmaceutics* 191, 1-14.
- Lee, D.B., Mixture, S., Kwon, H.C., Kwon, Y.P., Park, S., Lee, J.C., 2009. Effect of nano-coating on the thermal conductivity of microporous thermal insulations. *Journal of the Korean Physical Society* 54, 1119-1122.
- Lee, J.S., Kim, B.K., Kim, K.H., Park, D.J., 2008. Preparation of Low-Fat Uptake Doughnut by Dry Particle Coating Technique. *Journal of food science* 73, E137-E142.
- Lefebvre, G., Galet, L., Chamayou, A., 2011. Dry coating of talc particles with fumed silica: Influence of the silica concentration on the wettability and dispersibility of the composite particles. *Powder Technology* 208, 372-377.
- Li, Q., Rudolph, V., Weigl, B., Earl, A., 2004. Interparticle van der Waals force in powder flowability and compactibility. *International Journal of Pharmaceutics* 280, 77-93.
- Mohan, M.R., Dave, R.N., Pfeffer, R., 2003a. Promotion of deactivated sintering by dry-particle coating. *AIChE Journal* 49, 604-618.
- Mohan, M.R., Dave, R.N., Pfeffer, R., 2003b. Promotion of deactivated sintering by dry-particle coating. *AIChE Journal* 49, 604-618.
- Molerus, O., Nywlt, M., 1984. The influence of the fine particle content of the flow behaviour of bulk materials. *Powder Technology* 37, 145-154.
- Mujumdar, A., Wei, D., Dave, R.N., Pfeffer, R., Wu, C.Y., 2004. Improvement of humidity resistance of magnesium powder using dry particle coating. *Powder Technology* 140, 86-97.

- Mullarney, M.P., Beach, L.E., Davé, R.N., Langdon, B.A., Polizzi, M., Blackwood, D.O., 2011a. Applying dry powder coatings to pharmaceutical powders using a comil for improving powder flow and bulk density. *Powder Technology* 212, 397-402.
- Mullarney, M.P., Beach, L.E., Langdon, B.A., Polizzi, M.A., 2011b. Applying dry powder coatings: Using a resonant acoustic mixer to improve powder flow and bulk density. *Pharmaceutical Technology* 35, 94-102.
- Nagata, K., Okamoto, H., Danjo, K., 2001. Naproxen particle design using porous starch. *Drug Development and Industrial Pharmacy* 27, 287-296.
- Naito, M., Kondo, A., Yokoyama, T., 1993. Applications of comminution techniques for the surface modification of powder materials. *ISIJ international* 33, 915-924.
- Naito, M., Yoshikawa, M., Yotsuya, T., 1990. Preparation of superconducting oxide by a new attrition type mill. *Funtai Oyobi Fummatsu Yakin/Journal of the Japan Society of Powder and Powder Metallurgy* 37, 131-133.
- Nakane, T., Koishi, M., Fukui, H., Okunuki, Y., Yahata, Y., Kumagai, S., Yokoyama, H., Yagi, E., Fukuda, M., Ohta, T., 1992. Composite powder and production process. Google Patents.
- Narayanan, A., Sharma, P., Moudgil, B.M., 2013. Applications of Engineered Particulate Systems in Agriculture and Food Industry. *KONA Powder and Particle Journal* 30, 221-235.
- Narh, K.A., Agwedicham, A.T., Jallo, L., 2008. Dry coating polymer powder particles with deagglomerated carbon nanotubes to improve their dispersion in nanocomposites. *Powder Technology* 186, 206-212.
- Nase, S.T., Vargas, W.L., Abatan, A.A., McCarthy, J.J., 2001. Discrete characterization tools for cohesive granular material. *Powder Technology* 116, 214-223.
- Ning, G., Li, P., Zhang, T., Zhou, Z., Li, D., 2013. Hydrophobic nano-silica for the surface modification of graphite flake. *Propellants, Explosives, Pyrotechnics* 38, 520-524.
- Ogawa, K., Takata, S., Nanba, T., Yoshino, K., 2000. Powder coated with sparingly soluble ultraviolet absorber. Google Patents.
- Okawa, H., Lee, J.H., Hotta, T., Ohara, S., Takahashi, S., Shibahashi, T., Yamamasu, Y., 2004. Performance of NiO/MgFe₂O₄ composite cathode for a molten carbonate fuel cell. *Journal of Power Sources* 131, 251-255.
- Ouabbas, Y., Chamayou, A., Galet, L., Baron, M., Thomas, G., Grosseau, P., Guilhot, B., 2009a. Surface modification of silica particles by dry coating: Characterization and powder ageing. *Powder Technology* 190, 200-209.
- Ouabbas, Y., Dodds, J., Galet, L., Chamayou, A., Baron, M., 2009b. Particle–particle coating in a cyclomix impact mixer. *Powder Technology* 189, 245-252.
- Pearnchob, N., Bodmeier, R., 2003a. Coating of pellets with micronized ethylcellulose particles by a dry powder coating technique. *International journal of pharmaceutics* 268, 1-11.

- Pearnchob, N., Bodmeier, R., 2003b. Dry polymer powder coating and comparison with conventional liquid-based coatings for Eudragit® RS, ethylcellulose and shellac. *European journal of pharmaceuticals and biopharmaceutics* 56, 363-369.
- Pfeffer, R., Dave, R.N., Wei, D., Ramlakhan, M., 2001a. Synthesis of engineered particulates with tailored properties using dry particle coating. *Powder Technology* 117, 40-67.
- Pfeffer, R., Dave, R.N., Wei, D., Ramlakhan, M., 2001b. Synthesis of engineered particulates with tailored properties using dry particle coating. *Powder Technology* 117, 40-67.
- Poux, M., Fayolle, P., Bertrand, J., Bridoux, D., Bousquet, J., 1991. Powder mixing: some practical rules applied to agitated systems. *Powder Technology* 68, 213-234.
- Rabinovich, Y.I., Adler, J.J., Ata, A., Singh, R.K., Moudgil, B.M., 2000. Adhesion between nanoscale rough surfaces: I. Role of asperity geometry. *Journal of Colloid and Interface Science* 232, 10-16.
- Ramlakhan, M., Wu, C.Y., Watano, S., Dave, R.N., Pfeffer, R., 2000. Dry particle coating using magnetically assisted impaction coating: Modification of surface properties and optimization of system and operating parameters. *Powder Technology* 112, 137-148.
- Reynolds, G.K., 2010. Modelling of pharmaceutical granule size reduction in a conical screen mill. *Chemical Engineering Journal* 164, 383-392.
- Rietema, K., 1991. *The dynamics of fine powders*. Springer Science & Business Media.
- Rumpf, H., Bull, F., 1990. *Particle technology*. Chapman and Hall London.
- Sallam, E., Badwan, A., Takiuddin, M., 1986. Surface Characterisation of Sucrose and Antibiotics Powder Mixes with Relevance to Mixing Theories. *Drug Development and Industrial Pharmacy* 12, 1731-1748.
- Sato, A., Serris, E., Grosseau, P., Thomas, G., Chamayou, A., Galet, L., Baron, M., 2012. Effect of operating conditions on dry particle coating in a high shear mixer. *Powder Technology* 229, 97-103.
- Simner, S.P., Anderson, M.D., Coleman, J.E., Stevenson, J.W., 2006. Performance of a novel La(Sr)Fe(Co)O₃-Ag SOFC cathode. *Journal of Power Sources* 161, 115-122.
- Simner, S.P., Anderson, M.D., Templeton, J.W., Stevenson, J.W., 2007. Silver-perovskite composite SOFC cathodes processed via mechanofusion. *Journal of Power Sources* 168, 236-239.
- Simner, S.P., Templeton, J.W., Stevenson, J.W., 2008. Electrochemical characterization of modified LSM cathodes, *Ceramic Engineering and Science Proceedings*, 4 ed, pp. 167-175.
- Singh, R., Ata, A., Fitz-Gerald, J., Hendrickson, W., 1997. Dry coating method for surface modification of particulates. *Surface engineering* 13, 295-298.

- Smikalla, M., Mescher, A., Walzel, P., Urbanetz, N.A., 2011. Impact of excipients on coating efficiency in dry powder coating. *International journal of pharmaceutics* 405, 122-131.
- Suda, Y., Yoshida, M., Kawai, E., Mugikura, S., 2006. Oily skin preparation for external use. Google Patents.
- Tanno, K., Onagi, T., Naito, M., 1994. Preparation of stainless steel/zirconia composite particles with a multi-phase coating layer. *Advanced Powder Technology* 5, 393-405.
- Tay, T., Morton, D.A.V., Gengenbach, T.R., Stewart, P.J., 2012. Dissolution of a poorly water-soluble drug dry coated with magnesium and sodium stearate. *European Journal of Pharmaceutics and Biopharmaceutics* 80, 443-452.
- Teng, S., Wang, P., Zhu, L., Young, M.-W., Gogos, C.G., 2009. Experimental and numerical analysis of a lab-scale fluid energy mill. *Powder Technology* 195, 31-39.
- Thalberg, K., Lindholm, D., Axelsson, A., 2004. Comparison of different flowability tests for powders for inhalation. *Powder Technology* 146, 206-213.
- Ukita, K., Kuroda, M., Honda, H., Koishi, M., 1989. Characterization of powder-coated microspunge prepared by dry impact blending method. *Chemical and pharmaceutical bulletin* 37, 3367-3371.
- Umakoshi, M., Ito, H., Nakamura, R., Yokoyama, T., Urayama, K., Kato, M., 1993. Properties of the Ni-Al composite powders prepared by the mechanofusion process and their plasma sprayed coatings. *Funtai Oyobi Fumatsu Yakin/Journal of the Japan Society of Powder and Powder Metallurgy* 40, 241-246.
- Vasilenko, A., Glasser, B.J., Muzzio, F.J., 2011. Shear and flow behavior of pharmaceutical blends — Method comparison study. *Powder Technology* 208, 628-636.
- Vilela, A., Concepcion, L., Accart, P., Chamayou, A., Baron, M., Dodds, J.A., 2006. Evaluation of the Mechanical Resistance of a Powder-powder Coating by Modulated Dry Feed Particle Size Analysis. *Particle & Particle Systems Characterization* 23, 127-132.
- Wada, M., Yoshinaga, H., Kajita, O., Sakai, T., Irikawa, M., Miyamura, H., Kuriyama, N., Uehara, I., 1993. Production of copper-alloy complex granules for nickel/metal hydride electrodes. *Journal of Alloys and Compounds* 192, 164-166.
- Watano, S., Imada, Y., Miyanami, K., Wu, C.-Y., Dave, R.N., Pfeffer, R., Yoshida, T., 2000. Surface Modification of Food Fiber by Dry Particle Coating. *Journal of chemical engineering of Japan* 33, 848-854.
- Watano, S., Nakamura, H., Hamada, K., Wakamatsu, Y., Tanabe, Y., Dave, R.N., Pfeffer, R., 2004. Fine particle coating by a novel rotating fluidized bed coater. *Powder Technology* 141, 172-176.
- Wei, D., Dave, R., Pfeffer, R., 2002. Mixing and characterization of nanosized powders: an assessment of different techniques. *Journal of Nanoparticle Research* 4, 21-41.

- Xie, H.Y., 1997. The role of interparticle forces in the fluidization of fine particles. *Powder Technology* 94, 99-108.
- Yang, J., Sliva, A., Banerjee, A., Dave, R.N., Pfeffer, R., 2005. Dry particle coating for improving the flowability of cohesive powders. *Powder Technology* 158, 21-33.
- Yokoyama, T., Urayama, K., Naito, M., Kato, M., Yokoyama, T., 1987. The angmill mechanofusion system and its applications. *KONA Powder and Particle Journal* 5, 59-68.
- Yokoyama, T., Urayama, K., Yokoyama, T., 1983. Ultra-Fine Grinding and Consequent Changes of Powder Characteristics. *KONA Powder and Particle Journal* 1, 53-63.
- Yoshida, H., Lu, Y., Nakayama, H., Hirohashi, M., 2009. Fabrication of TiO₂ film by mechanical coating technique and its photocatalytic activity. *Journal of Alloys and Compounds* 475, 383-386.
- Young, M.-W., Gogos, C.G., Yang, J., Dave, R., Zhu, L., Bonnett, P., Schepige, W., 2012. Continuous high-speed coating of finely ground particulates. Google Patents.
- Zhang, Q., Wang, P., Teng, S., Qian, Z., Zhu, L., Gogos, C.G., 2010. Simultaneous milling and coating of inorganic particulates with polymeric coating materials using a fluid energy mill. *Polymer Engineering & Science* 50, 2366-2374.
- Zhou, Q., Armstrong, B., Larson, I., Stewart, P.J., Morton, D.A.V., 2010a. Improving powder flow properties of a cohesive lactose monohydrate powder by intensive mechanical dry coating. *Journal of Pharmaceutical Sciences* 99, 969-981.
- Zhou, Q., Qu, L., Gengenbach, T., Larson, I., Stewart, P.J., Morton, D.A.V., 2013a. Effect of surface coating with magnesium stearate via mechanical dry powder coating approach on the aerosol performance of micronized drug powders from dry powder inhalers. *AAPS PharmSciTech* 14, 38-44.
- Zhou, Q., Shi, L., Marinaro, W., Lu, Q., Sun, C.C., 2013b. Improving manufacturability of an ibuprofen powder blend by surface coating with silica nanoparticles. *Powder Technology* 249, 290-296.
- Zhou, Q.T., Qu, L., Gengenbach, T., Larson, I., Stewart, P.J., Morton, D.A., 2013c. Effect of surface coating with magnesium stearate via mechanical dry powder coating approach on the aerosol performance of micronized drug powders from dry powder inhalers. *AAPS PharmSciTech* 14, 38-44.
- Zhou, Q.T., Qu, L., Larson, I., Stewart, P.J., Morton, D.A., 2010b. Improving aerosolization of drug powders by reducing powder intrinsic cohesion via a mechanical dry coating approach. *International journal of pharmaceutics* 394, 50-59.
- Zhou, Q.T., Qu, L., Larson, I., Stewart, P.J., Morton, D.A.V., 2010c. Improving aerosolization of drug powders by reducing powder intrinsic cohesion via a mechanical dry coating approach. *International Journal of Pharmaceutics* 394, 50-59.

Zhou, Q.T., Qu, L., Larson, I., Stewart, P.J., Morton, D.A.V., 2011. Effect of mechanical dry particle coating on the improvement of powder flowability for lactose monohydrate: A model cohesive pharmaceutical powder. *Powder Technology* 207, 414-421.